

## Forum Original Research Communication

# The Plasma Membrane Is the Site of Selective Phosphatidylserine Oxidation During Apoptosis: Role of Cytochrome *c*

YULIA Y. TYURINA,<sup>1,3,4</sup> KAZUAKI KAWAI,<sup>1,4</sup> VLADIMIR A. TYURIN,<sup>1,3</sup> SHANG-XI LIU,<sup>1</sup>  
VALERIAN E. KAGAN,<sup>1,2</sup> and JAMES P. FABISIAK<sup>1</sup>

### ABSTRACT

Phosphatidylserine (PS) externalization, a functional end point of apoptosis that triggers phagocytic recognition of dying cells, may be modulated by oxidative stress in biological membranes. We previously observed selective oxidation of PS during apoptosis, but the intracellular location and molecular mechanisms responsible for PS oxidation remain to be described. Peroxidation in individual classes of cellular phospholipids was monitored in whole cells and various subcellular fractions obtained from HL-60 cells undergoing apoptosis in response to *tert*-butyl hydroperoxide (*t*-BuOOH) after metabolic acylation of phospholipids with the oxidation-sensitive fluorescent fatty acid, *cis*-parinaric acid. Nonrandom selective oxidation of PS was observed in whole cells, as well as in plasma membrane. PS in mitochondria appeared selectively resistant to oxidation during apoptosis. All phospholipids in nuclear membranes appeared resistant to oxidation after *t*-BuOOH treatment. Selective PS oxidation was accompanied by cytochrome *c* release and PS externalization. PS oxidation and externalization were followed by caspase activation and other end points of apoptosis. HL-60 cells “loaded” with exogenous cytochrome *c* by mild sonication showed selective oxidation of PS in both the absence and presence of *t*-BuOOH. Cytochrome *c*/hydrogen peroxide could effectively oxidize purified PS but not phosphatidylcholine in a cell-free model system. Selective plasma membrane-based PS oxidation and subsequent externalization during oxidant-induced apoptosis may be mediated through the redox activity of cytochrome *c*. *Antioxid. Redox Signal.* 6, 209–225.

### INTRODUCTION

APOPTOSIS, OR PROGRAMMED CELL DEATH, is essential for normal tissue development, immunologic selection, and response to tissue injury. Apoptosis permits the orderly elimination of cells when they are damaged beyond repair or no longer functionally required (28). Several biochemical and morphological end points of apoptosis have been described, includ-

ing chromatin condensation and fragmentation, internucleosomal DNA cleavage, and redistribution of plasma membrane phospholipids (1). This latter effect, typified by the disruption of normal plasma membrane phospholipid asymmetry and relocation of phosphatidylserine(PS) to the external surface, serves an important role to signal recognition, phagocytosis, and elimination of apoptotic cells by macrophages, thus minimizing inflammation during apoptosis (68). The early externalization

<sup>1</sup>Department of Environmental and Occupational Health, Graduate School of Public Health, and <sup>2</sup>Department of Pharmacology, School of Medicine, University of Pittsburgh, Pittsburgh, PA.

<sup>3</sup>Drs. Tyurina and Tyurin are on leave from Institute of Evolutionary Physiology and Biochemistry, Russian Academy of Science, St. Petersburg, Russia.

<sup>4</sup>Drs. Tyurina and Kawai contributed equally to this study.

of PS on the surface of the cell membrane appears to be an almost universal phenomenon in cells undergoing apoptosis (22, 44), although several instances of apoptosis in the absence of PS exposure have also been observed (21, 24, 36, 37).

The execution of apoptosis requires the active initiation and propagation of specific biochemical events that give rise to the end points described above. Several processes, including changes in mitochondrial permeability transition (41, 53, 81), release of cytochrome *c* from mitochondria to cytosol (31, 40, 61, 80), and caspase activation (17, 51), have been specifically assigned to the execution of apoptosis. Aminophospholipid translocase (APT) is a membrane-bound enzyme whose normal role is to transport aminophospholipids from the outer to the inner monolayer of plasma membrane (8, 16, 79). Inhibition of the surveillance function of this enzyme during apoptosis is considered a prerequisite for PS externalization in plasma membrane (43). Activation of phospholipid scramblase, another membrane-bound enzyme that transports multiple phospholipids, including PS, in both directions is also probably important for the occurrence of PS externalization (7). The factors that govern the regulation of these plasma membrane-localized processes during apoptosis and their precise relationship to mitochondrial changes and caspase activation remain to be described.

Oxidative stress, in general, and lipid peroxidation, in particular, have been implicated as part of the final common pathway of apoptosis (10, 13, 38, 60). We have previously shown that selective oxidation of PS in cells was an early event during apoptosis, preceded PS externalization, and was inhibited by overexpression of the antiapoptotic gene, *bcl-2* (18). These observations have led us to speculate that selective oxidation of PS occurs by an apoptosis-dependent mechanism different from random oxidative stress and that PS oxidation may, in some way, participate in its subsequent externalization within the membrane. This idea is supported by the fact that selective oxidation of PS during apoptosis was resistant to protection by the vitamin E analogue, 6-hydroxy-2,2,5,7,8-pentamethylchromane (19).

One important prediction of this hypothesis is that selective oxidation of PS occurs in the plasma membrane, where oxidized PS on the external surface of the plasma membrane may be a preferred ligand for receptor interaction with phagocytic macrophages (36, 37). In addition, the APT is sensitive to oxidative and nitrosative modification of its SH groups (14, 20, 29), and it is therefore tempting to speculate that oxidative stress may also play a role in translocase inhibition and the subsequent loss of phospholipid asymmetry. Either oxidized PS may fail to be recognized by APT, and thus escape its surveillance function, or reactive oxidative products of PS may covalently modify APT within the active/catalytic site and serve to "poison" the enzyme.

Here we show that apoptosis following exposure of HL-60 cells to the oxidant, *tert*-butyl hydroperoxide (*t*-BuOOH), is accompanied by selective oxidation of PS. We examined the subcellular localization of PS oxidation and observed that most of this oxidation of PS occurs within the plasma membrane. We further hypothesized that PS oxidation would be coincident with the mitochondrial release of the potentially redox-active hemoprotein, cytochrome *c*; therefore, we also examined the ability of cytochrome *c* itself to mediate selective oxidation of PS.

## MATERIALS AND METHODS

### Reagents

All tissue culture media (RPMI-1640 and L-15) and additives were obtained from GibcoBRL (Gaithersburg, MD, U.S.A.) except fetal bovine serum, which was from Sigma (St. Louis, MO, U.S.A.). Fatty acid-free human serum albumin (hSA), butylated hydroxytoluene, cytochrome *c* purified from horse heart, dithiothreitol, phenylmethylsulfonyl fluoride (PMSF), antipain, Ponceau S, and Hoechst 33258 and 33342 dyes were also from Sigma. 1-Palmitoyl-2-arachidonoyl-*sn*-glycero-3-phosphocholine and 1-palmitoyl-2-arachidonoyl-*sn*-glycero-3-phospho-L-serine were from Avanti Polar Lipids (Alabaster, AL). Chloroform, hexane (HPLC grade), 2-propanol (HPLC grade), and Tween 20 were purchased from Aldrich Chemical Co. (Milwaukee, WI, U.S.A.). *cis*-Parinaric acid (PnA) was purchased from Molecular Probes, Inc. (Eugene, OR, U.S.A.). The purity of each lot of PnA was determined by UV spectrometry using the molar extinction  $\epsilon_{304} = 80 \text{ mM}^{-1} \text{ cm}^{-1}$  in ethanol. Anti-cytochrome *c* monoclonal antibody (clone 7H8.2C12) and secondary horseradish peroxidase-conjugated goat anti-mouse IgG-specific polyclonal antibody were obtained from PharMingen (San Diego, CA, U.S.A.). The caspase-3 assay kit was from Clontech (Palo Alto, CA, U.S.A.). Polyacrylamide, sodium dodecyl sulfate, and nitrocellulose membrane were purchased from Bio-Rad (Hercules, CA, U.S.A.). SuperSignal™ West Pico chemiluminescence assay system was from Pierce Chemical (Rockford, IL, U.S.A.). Pepstatin A, leupeptin, and Liqui-gel were purchased from ICN Biochemicals, Inc. (Aurora, OH, U.S.A.). Proteinase K, ribonuclease (RNase) T1, and RNase A were from Boehringer-Mannheim (Indianapolis, IN, U.S.A.). All other chemicals and reagents were molecular biology grade.

### Cell culture and treatment

HL-60 cells were grown in RPMI 1640 medium supplemented with 12% fetal bovine serum at 37°C under 5% CO<sub>2</sub> atmosphere. The density of cells at time of collection was  $0.5 \times 10^6$ – $1.0 \times 10^6$  cells/ml. Cells were rinsed once with L-15 medium supplemented with glucose (2 mg/ml) (pH 7.4), resuspended in the same medium to give a final cell density of  $2 \times 10^6$  cells/ml. Cells were then incubated (37°C) in the presence or absence of *t*-BuOOH (150  $\mu\text{M}$ ) for the indicated times after which cells were collected for various assays. For the analysis of early lipid peroxidation events, BHT (10  $\mu\text{M}$ ) was added after 20 min of incubation in order to quench *t*-BuOOH action and prevent lipid peroxidation during isolation of subcellular fractions. Cells were incubated an additional 40 min prior to harvest. In the experiments utilizing cytochrome *c*, the protein was incorporated into cells as described below before addition of *t*-BuOOH.

### Incorporation of cytochrome *c* into HL-60 cells

Cytochrome *c* was incorporated into HL-60 cells by mild sonication. Cells ( $1 \times 10^7$  cells/ml) were suspended in 25 mM HEPES buffer (pH 7.4) containing 115 mM NaCl, 5 mM KCl, 1 mM MgCl<sub>2</sub>, 5 mM NaH<sub>2</sub>PO<sub>4</sub>, and 10 mM glucose. Cells were then gently sonicated in an FS3 water bath sonicator (Fisher Scientific, Pittsburgh, PA, U.S.A.) for 8 s at 4°C in the presence of 1 mM cytochrome *c*. After sonication, the

cells were incubated for an additional 10 min at 37°C. Cells were then centrifuged at 1,000 *g* for 10 min and washed twice with 25 mM HEPES buffer (pH 7.4), and the amount of incorporated cytochrome *c* was determined spectrophotometrically using  $\epsilon_{553}^{\text{red}} = 15.3 \times 10^3 \text{ M}^{-1} \text{ cm}^{-1}$  (9). Viability of cells after these procedures was >95% as judged by Trypan Blue exclusion. For lipid peroxidation experiments using these cells, the percentage of PnA oxidation was determined relative to control cells that were sonicated in the absence of cytochrome *c*.

### *Nuclear morphology and DNA cleavage*

Nuclear morphology was assessed using Hoescht 33342 fluorescent staining as previously described (18, 19). The percentage of apoptotic cells was determined by counting at least 300 cells scored as either normal or apoptotic. Apoptotic nuclei were identified based upon their characteristic condensed and fragmented appearance.

Low-molecular-weight DNA fragmentation was determined using conventional gel electrophoresis as described previously (18, 19). Aliquots of  $1 \times 10^6$  cells were collected after treatment. Cell pellets were lysed and digested with Proteinase K (1 mg/ml, final concentration) followed by RNase A and RNase T1. Samples were electrophoresed in 2% agarose gels, stained with ethidium bromide, and evaluated under UV illumination.

### *Cytochrome c release from mitochondria in HL-60 cells*

*t*-BuOOH-treated HL-60 cells were harvested by centrifugation at 700 *g* for 10 min. The cell pellets were resuspended with buffer containing 20 mM HEPES-KOH (pH 7.5), 10 mM KCl, 1.5 mM MgCl<sub>2</sub>, 1 mM sodium EDTA, 1 mM sodium EGTA, 1 mM dithiothreitol, 0.1 mM PMSF, and 250 mM sucrose. The cells were homogenized with 10 strokes of a Potter-Elvehjem homogenizer, and the homogenates were centrifuged at 700 *g* for 10 min. The supernatants were centrifuged at 100,000 *g* for 1 h at 4°C, and the resulting pellets and supernatants were used for cytochrome *c* measurement by western blotting.

Samples containing 10 µg of protein were separated on 12% sodium dodecyl sulfate–polyacrylamide gel electrophoresis gels and transferred to nitrocellulose membranes (0.2 µm; Bio-Rad). Ponceau S staining was applied to verify that an equal amount of protein was present in each lane. The membranes were blocked with 5% nonfat milk in 50 mM Tris-HCl (pH 7.5), 200 mM NaCl, 0.05% Tween 20 for 1 h and subsequently exposed to primary anti-cytochrome *c* antibody (1:100). After washing, the membranes were exposed to horseradish peroxidase-linked goat anti-mouse IgG secondary antibody (PharMingen) for 1 h. Cytochrome *c* bands were visualized using the SuperSignal West Pico chemiluminescence assay system (Pierce Chemical) and exposure to autoradiographic film. Image capture and subsequent analyses were performed using Fluor-S MultiImager (Bio-Rad) and Multi-Analyst Software (Bio-Rad).

### *Subcellular fractionation*

*Isolation of mitochondria, microsomes, plasma membrane, and lysosomes.* HL-60 cells metabolically

labeled with PnA (see below) were incubated with or without *t*-BuOOH as described below and washed once with serum-free L-15 medium supplemented with glucose. Cells ( $1 \times 10^8$  cells/ml) were disrupted by homogenization for 5 min at 4°C in hypotonic buffer containing 10 mM Tris-HCl (pH 7.4), 5 mM NaCl, 5 mM KCl, and 2 mM EDTA (5 strokes/min) in a glass/Teflon homogenizer. Cell lysis was confirmed by examination under a microscope. After disruption, the homogenate was immediately combined with an equal volume of 30 mM Tris-HCl buffer (pH 7.4) containing 195 mM NaCl, 5 mM KCl, 2 mM EDTA, and 0.5 M sucrose in order to achieve a final concentration of 0.25 M sucrose, 20 mM Tris-HCl, 100 mM NaCl, 5 mM KCl, and 2 mM EDTA. Unbroken cells and nuclei were separated by centrifugation at 1,000 *g* for 7 min at 4°C. The crude mitochondrial fraction, containing plasma membrane, mitochondria, and lysosomes, was isolated from postnuclear supernatant by centrifugation at 12,000 *g* for 10 min at 4°C. Supernatant obtained after this centrifugation was used for isolation of microsomes by centrifugation at 100,000 *g* for 1 h at 4°C. Plasma membranes were isolated from the crude mitochondrial fraction by centrifugation over a discontinuous sucrose gradient (0.6–1.0 M) at 50,000 *g* for 1 h at 4°C. After centrifugation, fractions of plasma membrane and mitochondria/lysosomes were collected at the 0.8 M and 1.0 M layers of sucrose, respectively. Mitochondria were isolated from lysosomes in a single 30-min centrifugation at 50,000 *g* using a hybrid Percoll-metrazamide gradient as described by Storrie and Madden (72). For high-speed ultracentrifugations, an L7 centrifuge (Beckman Instruments, Inc., Fullerton, CA, U.S.A.) equipped with fixed-angle and swinging bucket rotors was used for nongradient and gradient centrifugations, respectively.

*Isolation of nuclei.* Nuclei were separated from the crude nuclear fraction by centrifugation as described by Ishikura *et al.* (30). Unbroken cells and nuclei were washed once with hypotonic buffer containing 10 mM Tris-HCl (pH 7.9), 24 mM KCl, 10 mM MgCl<sub>2</sub>, and 1 mM dithiothreitol. After centrifugation, the pellet was suspended in hypotonic buffer, kept on ice for 5 min, and then homogenized (10 strokes) in a glass/Teflon homogenizer. Nuclei were collected by centrifugation at 1,000 *g* for 7 min at 4°C, washed once in hypotonic buffer, and suspended in buffer containing 40% glycerol, 20 mM HEPES (pH 7.6), 2 mM MgCl<sub>2</sub>, and 2 mM dithiothreitol. Nuclei were purified by centrifugation through 2.2 M sucrose in 5 mM Tris-HCl (pH 7.0) containing 5 mM MgCl<sub>2</sub> at 50,000 *g* for 1 h at 4°C.

### *Characterization of subcellular fractions*

Assays for a variety of organelle-specific marker enzymes were performed as described below. Analysis of the plasma membrane marker, Na<sup>+</sup>, K<sup>+</sup>-ATPase, was performed as described previously (30). NADPH cytochrome *c* reductase activity, a microsomal marker, was measured spectrophotometrically (32). Succinate nitroxide oxidoreductase for mitochondria was assayed using the free radical 2,2,6,6-tetramethylpiperidine-*N*-oxyl (TEMPO) as the electron acceptor and measuring the decrease of TEMPO signal intensity with electron paramagnetic resonance. The reaction mixture contained 0.1 mM succinate, 4 µM TEMPO, 1 mM KCN, 0.1 mM coenzyme Q<sub>0</sub>, and 1 mg of organelle protein per 82 µl in 30 mM phosphate buffer (pH 7.6). Lysosomal β-galactosidase activity was mea-

sured according to the procedure of Storrie and Madden (72) using 4-methylumbelliferyl- $\beta$ -D-galactopyranoside as a substrate. DNA was assayed fluorometrically using Hoechst 33258 (12). Protein concentration was measured by the Bradford assay (Bio-Rad) in 96-well microtiter plates using bovine serum albumin as a standard.

### Lipid peroxidation

**Incorporation of PnA into HL-60 cell phospholipids.** Cells were rinsed with L-15 medium supplemented with glucose (2 mg/ml) (pH 7.4). PnA was incorporated into HL-60 cell phospholipids by incubation of cells ( $2 \times 10^6$  cells/ml) in L-15 medium in the presence of PnA-hSA complex (2  $\mu$ g of PnA/ $10^6$  cells) for 2 h at 37°C in the dark under aerobic conditions. The complex was prepared as described previously (66). At the end of the incubation period, the cells were washed first with L-15 medium containing hSA (0.5 mg/ml) and then again with L-15 without hSA to remove unincorporated PnA. PnA-loaded cells were treated with *t*-BuOOH or loaded with cytochrome *c* as described above.

**Lipid extraction and high-performance thin-layer chromatography (HPTLC) analysis.** Total lipids were extracted from intact HL-60 cells or fractions of subcellular organelles using a slightly modified Folch procedure as previously described (34, 66). Lipid extracts were dissolved in 0.2 ml of 2-propanol/hexane/water (4:3:0.16, by volume). The phospholipid classes in the extracts were separated by two-dimensional HPTLC on silica G plates (5  $\times$  5 cm; Whatman). The plates were first developed with a solvent system consisting of chloroform/methanol/28% ammonium hydroxide (65:25:5, by volume). After the plate was dried with a forced air blower to remove the solvent, the plates were developed in the second dimension with a solvent system consisting of chloroform/acetone/methanol/glacial acetic acid/water (50:20:10:10:5, by volume). The phospholipids were visualized by exposure to iodine vapor. The phospholipid spots identified by iodine staining were scraped off the plates and transferred to tubes. Lipid phosphorus in total extracts as well as in the individual spots was determined using the method described by Bottcher *et al.* (6). The identity of each phospholipid was previously established by comparison with the  $R_f$  values measured using authentic standards.

**PnA oxidation in specific phospholipid classes.** Lipid extracts were separated by HPLC as previously described (34, 66). A 5-mm Supelcosil LC-Si column (4.6  $\times$  250 mm) equilibrated with a mixture of 1 part solvent A [2-propanol/hexane/water (57:43:1, by volume) and 9 parts solvent B [2-propanol/hexane/40 mM aqueous ammonium acetate (57:43:10)] (pH 6.7) was used for chromatography. The column was eluted during the first 3 min with a linear gradient from 10% solvent B to 37% solvent B. Isocratic elution with 37% solvent B was then performed for 12 min, followed by 8 min of a linear gradient from 37% to 100% solvent B. Lastly, the chromatography run was continued for 22 min with isocratic elution at 100% solvent B. A solvent flow rate was maintained at 1 ml/min throughout. The separations were performed using a Shimadzu HPLC (model LC-600; Kyoto, Japan) equipped with an in-line

configuration of fluorescence (model RF-551) and UV-VIS (model SPD-10AV) detectors. The effluent was monitored by fluorescence of PnA by emission at 420 nm after excitation at 324 nm. Fluorescence data were processed and stored in digital form with Shimadzu EZChrom software. The identity and location of specific phospholipids in the eluate were established by collecting each of the peak fractions and subjecting them to HPTLC analysis as described above. The PnA content of individual lipid species is expressed both relative to total lipid phosphorus recovered in the entire lipid fraction (relative activity) and relative to the amount of the specific phospholipid itself determined by parallel analysis by HPTLC (specific activity).

### Fluorescamine labeling of externalized aminophospholipids

Cells were labeled by fluorescamine as described by Fadok *et al.* (22). HL-60 cells ( $1 \times 10^8$ ) were suspended in 4 ml of fluorescamine labeling buffer [150 mM NaCl, 5 mM KCl, 1 mM  $MgCl_2$ , 1 mM  $CaCl_2$ , 5 mM  $NaHCO_3$ , 5 mM glucose, 20 mM HEPES (pH 8.0)]. Fluorescamine was dissolved in dimethyl sulfoxide and added to cells (200  $\mu$ M, final concentration). The mixture was gently shaken for 30 s at room temperature after which 4.5 ml of 40 mM Tris-HCl (pH 7.4) containing 100 mM NaCl was added and cells were centrifuged at 1,000 g for 10 min. The cell pellet was resuspended in 3 ml of 40 mM Tris-HCl buffer (pH 7.4), and lipids were extracted as described above. Lipids were analyzed by two-dimensional HPTLC as described above. Individual spots corresponding to fluorescamine-modified PS and phosphatidylethanolamine (PE) (mPS and mPE) were localized by exposing the plate to UV light, and unmodified phospholipids were visualized following exposure of the plate to iodine vapor. PS, mPS, PE, and mPE spots were scraped from the plate, and the phosphorus content of each spot was determined as described above. The amount of derivatized mPS and mPE was expressed as a percentage of the total PS and PE (unmodified plus modified), respectively, recovered from the plate based on phosphorus assay.

### Oxidation of phosphatidylcholine (PC)/PS liposomes by cytochrome *c* in the presence of hydrogen peroxide ( $H_2O_2$ )

Multilamellar dispersions of 1-palmitoyl-2-arachidonoyl-*sn*-glycero-3-phosphocholine or 1-palmitoyl-2-arachidonoyl-*sn*-glycero-3-phospho-L-serine (2 mg/ml) were incubated in 50 mM phosphate buffer (pH 7.4) containing cytochrome *c* (5  $\mu$ M), ascorbate (500  $\mu$ M),  $H_2O_2$  (400  $\mu$ M), and deferoxamine (100  $\mu$ M) for 1 h at 37°C. At various times, aliquots of reaction mixtures were taken for phospholipid extraction by the Folch procedure as described above. The lipid oxidation products contained in phospholipid extracts were estimated spectrophotometrically at 232 nm and 205 nm using a Shimadzu UV-VIS spectrophotometer UV160U (Kyoto, Japan). The formation of conjugated dienes was estimated as the ratio of  $A_{232}/A_{205}$ .

### Statistical evaluation

Data are expressed as means  $\pm$  SEM. Changes in variables for different incubations were analyzed by either Student's *t* test (single comparisons) or one-way ANOVA for multiple

comparisons. If the ANOVA revealed significant changes, then multiple unpaired Student's *t* tests were performed to establish differences between various groups. Differences among means were considered significant when the value was  $p \leq 0.05$ .

## RESULTS

### *t*-BuOOH induces apoptosis in HL-60 cells

**Nuclear morphology.** Nuclear condensation and fragmentation is an established biomarker of apoptosis. These morphological changes can be observed as small, bright staining nuclei, often very rounded and sometimes fragmented into distinct sections. HL-60 cells were incubated with *t*-BuOOH (150  $\mu$ M), and nuclear morphology at various times was then assessed by Hoechst 33342 staining. HL-60 cells treated with *t*-BuOOH acquired a nuclear phenotype characterized by chromatin condensation and fragmentation typical of apoptosis. This apoptotic morphology was observed in nearly 20% of the cells after 2 h of *t*-BuOOH exposure and increased to 79% 4 h after exposure (Fig. 1A).

**DNA fragmentation.** Another hallmark of apoptosis is the characteristic fragmentation of DNA into discrete fragments corresponding to internucleosomal cleavage (180–200 bp “ladders”). Figure 1B shows that treatment with *t*-BuOOH also induces internucleosomal DNA cleavage. DNA fragmentation could first be discerned following 2 h exposure to *t*-BuOOH, and the formation of 180–200 bp DNA “ladders” was clearly evident at 4 h post exposure. Internucleosomal DNA cleavage could not be observed at any time point in the control untreated cells.

**Caspase-3 activation in HL-60 cells.** Caspase-3 has been defined as a key proteolytic enzyme involved in the execution of apoptosis induced by many stimuli (46, 49, 51, 75). We, therefore, measured the ability of *t*-BuOOH to induce caspase-3 activity in HL-60 cells. Cell extracts were prepared at various times following treatment of HL-60 cells with *t*-BuOOH. Caspase-3 activity in cell extracts was determined by the cleavage of DEVD-AFC to yield the fluorescent product 7-amino-4-trifluoromethylcoumarin. As shown in Fig. 1C, *t*-BuOOH resulted in a time-dependent increase in caspase-3 activity in HL-60 cells. The activity after 2 h of exposure to *t*-BuOOH was about five times greater than that observed in extracts prepared from cells without treatment. A significant difference between control and *t*-BuOOH-treated cells could be observed as early as 1 h after treatment. A trend toward caspase-3 activation following incubation alone under serum-free conditions was observed; however, *t*-BuOOH produced significantly greater activation of caspase-3 as compared with control incubations at 1- and 2-h time points. Camptothecin, a well-known inducer of apoptosis in these cells, produced increments in caspase activity similar to *t*-BuOOH under these conditions (data not shown). These results indicate that apoptosis following *t*-BuOOH occurs concurrently with the activation caspase-3.

**Externalization of PS in HL-60 cells.** We next determined the ability of *t*-BuOOH to produce PS externaliza-

tion, another well-known biomarker of apoptosis. For this we utilized the chemical modification of externalized aminophospholipids by fluorescamine, a cell-impermeable reagent capable of reacting with primary amines. Following treatment, cell lipids were extracted and resolved by HPTLC as described in Materials and Methods. The distinct spots corresponding to fluorescamine-modified (mPE and mPS) and unmodified PS and PE were scraped, and determination of phosphorus content in these individual spots was performed. The amounts of mPE and mPS were quantified relative to the total PE and PS (modified plus unmodified), respectively. As shown in Fig. 1D, <1% of PS was accessible to fluorescamine on the surface of control untreated cells. Treatment with *t*-BuOOH (2 h), however, produced a 10-fold increase in the amount of PS available to fluorescamine. The amount of PE on the outer monolayer of cell membrane was not significantly different between untreated and treated cells and represented 10.7% and 11.8% of the total PE, respectively. Thus, marked specific externalization of the aminophospholipid, PS, occurs during *t*-BuOOH-induced apoptosis of HL-60 cells.

### *Release of cytochrome c from mitochondria.*

The release of cytochrome *c* from mitochondria is an early event in apoptotic cells, and it is known that caspase-3 is activated, in part, in a process that is dependent on release of cytochrome *c* from mitochondria (42, 61). We next determined whether *t*-BuOOH treatment results in the accumulation of the mitochondrial protein cytochrome *c* within the cytosol. Figure 2A shows a typical immunoblot used to detect cytochrome *c* in the cytosolic fractions obtained from HL-60 cells treated with *t*-BuOOH. Treatment with camptothecin (10  $\mu$ M) was used as a positive control in these experiments. The signal of 13-kDa cytochrome *c* was increased in the cytosol at 2 h following *t*-BuOOH treatment (lane 1, control; lane 2, *t*-BuOOH). Similar results were obtained following exposure to the positive control, camptothecin (lane 3). Quantitative analysis of three separate experiments (Fig. 2B) revealed a statistically significant accumulation of cytochrome *c* in cytosolic extracts corresponding to approximately a two-fold increase following *t*-BuOOH and three-fold increase following camptothecin. These data clearly show that apoptosis following treatment of HL-60 cells with *t*-BuOOH is accompanied by the release of cytochrome *c* from mitochondria to cytoplasm.

### *Phospholipid oxidation during t-BuOOH-induced apoptosis*

To assess site-specific oxidation of phospholipids during oxidant-induced apoptosis, we used our previously described method based on metabolic incorporation of the oxidation-sensitive fluorescent fatty acid, PnA, into cellular phospholipids and assessment of fluorescence loss in individual phospholipid classes following resolution by HPLC (34, 66). This method provides an extremely sensitive way to measure low levels of lipid oxidation in specific phospholipid classes in live cells that is independent of various phospholipid repair mechanisms. Furthermore, we have now extended this assay here by using subcellular fractionation to ascertain in what particular cellular compartments various lipid oxidation events occur.

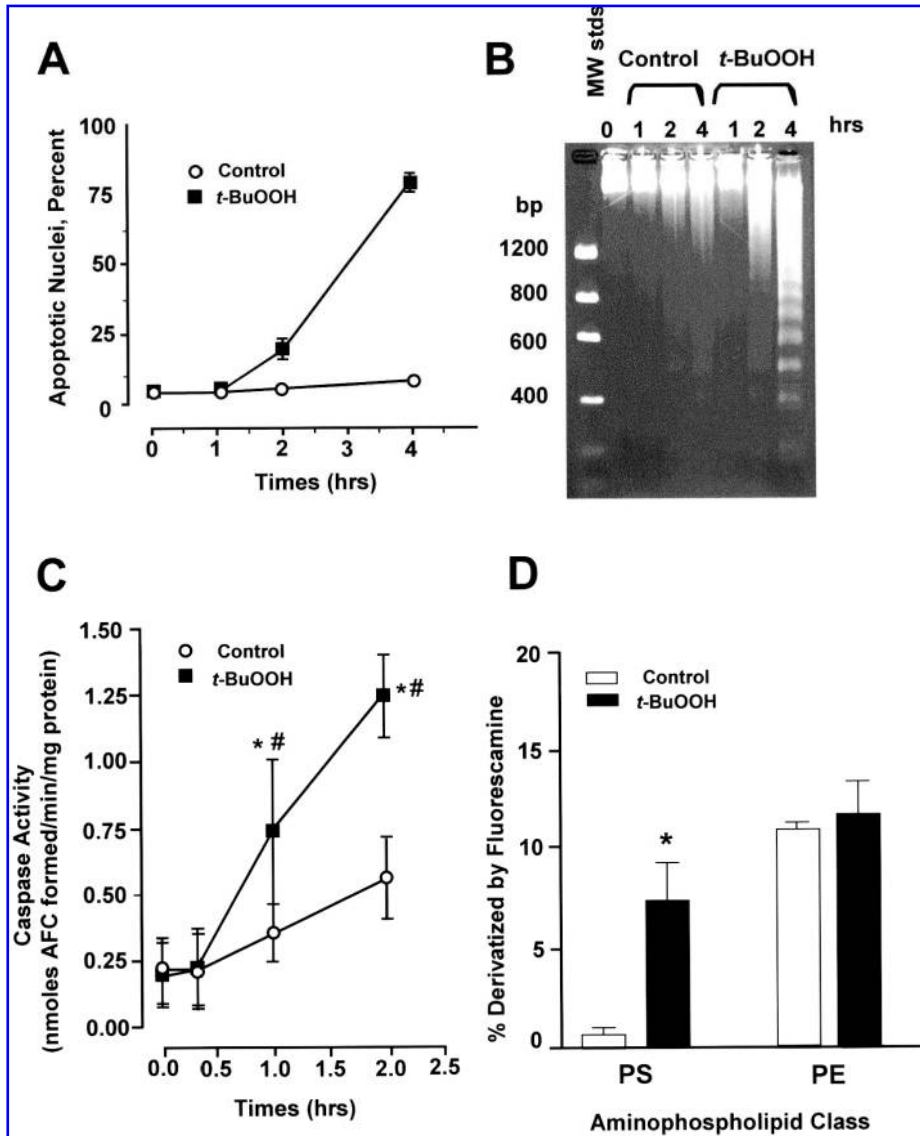


**FIG. 1. *t*-BuOOH apoptosis in HL-60 cells.** (A) *t*-BuOOH induced time-dependent formation of apoptotic nuclei in HL-60 cells. Cells were incubated in L-15 medium in the presence or absence of *t*-BuOOH (150  $\mu$ M) at 37°C for various times as indicated. Cells were stained using Hoescht 33342 and nuclei visualized as described in Materials and Methods. The percentage of cells with apoptotic nuclei typified by chromatin condensation and fragmentation was determined in at least 300 cells/sample. Data represent means  $\pm$  SEM obtained from three observations per time point. (B) *t*-BuOOH induced time-dependent appearance of internucleosomal DNA cleavage in HL-60 cells. Cells were incubated in L-15 medium in the presence or absence of *t*-BuOOH (150  $\mu$ M). Aliquots of cells were removed at various times and DNA was extracted as described in Materials and Methods. DNA samples corresponding to  $1 \times 10^6$  cells were subjected to gel electrophoresis in 2% agarose and then stained with ethidium bromide. Molecular-weight standards are included in the leftmost lane for reference. Note the time-dependent formation of 180–200 bp DNA “ladders” in the *t*-BuOOH-treated cells, but not in the control cells. Data represent a typical experiment that was repeated three times with essentially identical results. (C) *t*-BuOOH induces caspase-3 activation in HL-60 cells. HL-60 cells were treated with 150  $\mu$ M *t*-BuOOH in phenol red- and serum-free RPMI 1640 medium for 2 h at 37°C. Control cells were left untreated in the same media. Camptothecin (10  $\mu$ M) was used as positive control. Extracts from  $1 \times 10^6$  cells were prepared and assayed for caspase-3 activity using a commercially available kit (Clontech). Data represent means  $\pm$  SEM obtained from three separate experiments. Each experiment was performed using duplicate samples. \*Statistically significant difference ( $p < 0.05$ ) relative to time zero point and #statistically significant difference ( $p < 0.05$ ) relative to the same time point from untreated control by one-way ANOVA followed by Tukey’s multiple comparisons test. (D) Accessibility of PS and PE to fluorescamine following *t*-BuOOH treatment. HL-60 cells were incubated in the presence or absence of *t*-BuOOH (150  $\mu$ M) for 20 min at 37°C and then reacted with fluorescamine as described in Materials and Methods. The percentages of total PS and PE modified by fluorescamine were determined by phosphorus analysis of both the native and modified phospholipid spots after two-dimensional HPTLC. Data represent the means  $\pm$  SEM ( $n = 6$ ). \*Statistically significant difference ( $p < 0.005$ ) between treated and untreated cells by Student’s *t* test.

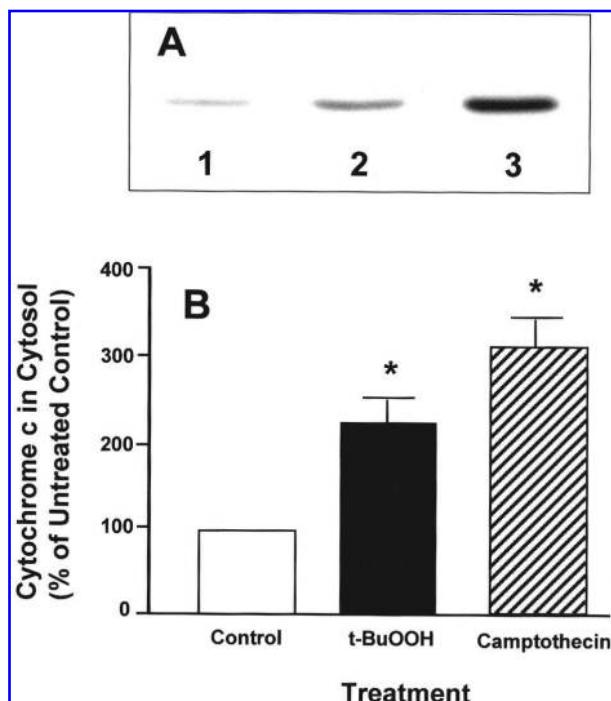


**FIG. 2. Mitochondrial release of cytochrome *c* release into cytosol following *t*-BuOOH.** (A) Typical immunoblot analysis of cytochrome *c* in cytosolic fractions isolated from HL-60 cells treated for 2 h with 150  $\mu$ M *t*-BuOOH (lane 2) and with 10  $\mu$ M camptothecin (lane 3), and nontreated control cells (lane 1). Camptothecin was used as positive control. (B) Quantification of the optical density of cytochrome *c* immunoblots. All data are means  $\pm$  SEM from three independent experiments, \* $p$  < 0.05 versus untreated control cells.

**Subcellular fractionation.** Various subcellular fractions were obtained as described in Materials and Methods. These included plasma membrane, mitochondria, microsomes, nuclei, and lysosomes. To assess the relative purity of these various fractions after isolation, we used the following enzyme activities as specific markers for various subcellular organelles: Na<sup>+</sup>/K<sup>+</sup>-ATPase for plasma membrane, NADPH cytochrome *c* reductase for microsomal fraction, succinate nitroxide oxidoreductase for mitochondria, and  $\beta$ -galactosidase for lyso-

somes. DNA content was also measured as a marker for nuclei. Table 1 shows the comparison of these various markers in the various subcellular fractions obtained following our isolation procedure. Na<sup>+</sup>/K<sup>+</sup>-ATPase was obviously enriched in the plasma membrane fraction where its specific activity (in nanomoles of NADH consumed per minute per milligram of protein) was ~50-fold greater than that observed in whole cells and 30-fold greater than that observed in the microsomal fraction. Trivial or no detectable Na<sup>+</sup>/K<sup>+</sup>-ATPase was observed in the remaining subcellular fractions. NADPH cytochrome *c* reductase was readily measured in the microsomal fraction (40.4 nmol of cytochrome *c* reduced/min/mg of protein) and enriched eight-fold compared with whole cell homogenates. NADPH cytochrome *c* reductase was not detected in the plasma membrane or nuclear fractions. Succinate nitroxide oxidoreductase could be detected only in the mitochondrial and microsomal fraction. The origin of this activity in the microsomal fraction could represent significant contamination of the microsomal fraction by mitochondria; however, there still remains a substantial difference in the expression of the microsomal marker, NADPH cytochrome *c* reductase, between these two fractions. In addition, DNA content, which could reflect, in part, the small pool of mitochondrial DNA within the cell, is 10-fold enriched in the mitochondrial fraction compared with microsomes. The bulk of DNA representing the nuclear chromatin content is clearly recovered in the nuclear fraction.  $\beta$ -Galactosidase, a lysosome marker, was relatively enriched in the lysosomal fraction compared with whole cell extracts (50.8 versus 4.4 nmol of 4-methylumbelliferone produced/min/mg of protein). Significant  $\beta$ -galactosidase could also be measured in the plasma membrane fraction (22.7 nmol of 4-methylumbelliferone produced/min/mg of protein) and presumably represents an incomplete separation of lysosomes from the plasma membrane fraction. We conclude from these enzymatic and DNA data that our subcellular fractionation procedure yielded fractions that were adequately enriched in plasma membrane, mitochondria, microsomes, nuclei, and lysosomes in order to be used to address the relative intracellular locations of specific phospholipid oxidations.

**Selective oxidation of PS during *t*-BuOOH apoptosis.** To determine if selective oxidation of PS occurred during apoptosis induced by *t*-BuOOH cells, metabolically la-

TABLE 1. CHARACTERIZATION OF SUBCELLULAR FRACTIONS OBTAINED FROM HL-60 CELLS

	Na <sup>+</sup> /K <sup>+</sup> -ATPase	NADPH cytochrome <i>c</i> reductase	Succinate nitroxide oxidoreductase	DNA	$\beta$ -galactosidase
Plasma membrane	102.5 $\pm$ 11.7	<0.5	<0.3	<0.02	22.7 $\pm$ 1.6
Mitochondria	0.1 $\pm$ 0.1	2.0 $\pm$ 0.1	13.3 $\pm$ 1.6	0.26 $\pm$ 0.02	1.5 $\pm$ 0.9
Microsomes	3.3 $\pm$ 2.0	40.4 $\pm$ 8.4	11.2 $\pm$ 4.6	0.03 $\pm$ 0.00	18.1 $\pm$ 1.5
Nuclei	<0.5	<0.5	<0.3	4.31 $\pm$ 0.47	8.1 $\pm$ 0.4
Lysosomes	<0.1	6.0 $\pm$ 6.0	<0.3	<0.02	50.8 $\pm$ 17.1
Intact cells	2.2 $\pm$ 2.2	5.2 $\pm$ 0.7	<0.3	0.09 $\pm$ 0.00	4.4 $\pm$ 0.3

Enzyme activities are expressed as specific activity defined, respectively: Na<sup>+</sup>/K<sup>+</sup>-ATPase, NADPH cytochrome *c* reductase, succinate nitroxide oxidoreductase,  $\beta$ -galactosidase, ouabain-sensitive nmol of NADH consumed/min/mg of protein; nmol of cytochrome *c* reduced/min/mg of protein; pmol of TEMPO reduced/min/mg of protein; nmol of 4-methylumbelliferone produced/min/mg of protein. DNA content is expressed as mg of DNA/mg of protein.

TABLE 2. PHOSPHOLIPID COMPOSITION OF INTACT CELLS AND VARIOUS SUBCELLULAR FRACTIONS ISOLATED FROM HL-60 CELLS

		DPG	PE	PC	SPH	PI	PS	LPC
Intact cells	Control	3.9 ± 0.3	27.4 ± 0.4	50.5 ± 0.9	5.9 ± 0.5	6.7 ± 0.3	5.1 ± 0.4	0.3 ± 0.1
	<i>t</i> -BuOOH	4.4 ± 0.2	26.7 ± 0.3	49.2 ± 0.3	6.9 ± 0.5	6.5 ± 0.5	5.6 ± 0.2	0.5 ± 0.1
Plasma membrane	Control	3.4 ± 0.4	30.1 ± 0.3	42.0 ± 1.2	9.9 ± 0.5	6.3 ± 0.9	8.2 ± 0.6	0.0 ± 0.0
	<i>t</i> -BuOOH	3.3 ± 0.6	31.9 ± 0.3	39.5 ± 1.7	11.3 ± 0.5	4.6 ± 0.5	7.9 ± 0.4	1.3 ± 0.3*
Mitochondria	Control	5.9 ± 0.2	26.9 ± 1.3	52.9 ± 0.6	2.8 ± 0.6	7.9 ± 0.6	3.1 ± 0.4	0.6 ± 0.2
	<i>t</i> -BuOOH	6.1 ± 0.4	27.7 ± 0.3	52.7 ± 1.2	3.6 ± 0.7	6.3 ± 0.8	1.8 ± 0.1	1.7 ± 0.8
Microsomes	Control	3.0 ± 0.3	27.3 ± 0.2	45.9 ± 0.8	8.8 ± 0.4	6.7 ± 0.3	7.6 ± 0.5	0.5 ± 0.1
	<i>t</i> -BuOOH	3.1 ± 0.3	27.8 ± 0.3	47.6 ± 1.3	8.8 ± 0.2	5.9 ± 1.0	6.0 ± 0.7	0.8 ± 0.1*
Nuclei	Control	1.9 ± 0.1	24.5 ± 0.4	64.9 ± 1.6	4.0 ± 0.3	6.1 ± 0.5	2.2 ± 0.1	0.0 ± 0.0
	<i>t</i> -BuOOH	2.4 ± 0.3	25.1 ± 0.6	59.3 ± 0.5	3.2 ± 0.3	6.6 ± 0.2	2.0 ± 0.3	1.4 ± 0.5*
Lysosomes	Control	7.2 ± 0.7	29.7 ± 1.1	42.0 ± 1.4	7.9 ± 0.4	6.6 ± 0.1	6.4 ± 0.3	0.4 ± 0.2
	<i>t</i> -BuOOH	6.6 ± 0.6	29.9 ± 1.2	37.5 ± 1.1	8.9 ± 0.7	7.6 ± 0.5	7.4 ± 0.7	1.9 ± 0.6

Data represent means ± SEM (*n* = 3) and are given as % of total phospholipids

\**p* < 0.05, compared with untreated control.

beled with PnA were treated with 150  $\mu$ M *t*-BuOOH for 20 min in L-15 medium supplemented with glucose. It was first important to determine if *t*-BuOOH induced any changes in the phospholipid content or distribution in HL-60 cells. Table 2 compares the relative distribution of various phospholipid classes derived from control and *t*-BuOOH-treated HL-60 cells. Two major phospholipids, PC and PE, represent about 50% and 25%, respectively, of the total phospholipids isolated from intact whole cells. The rank order of abundance for other phospholipids is phosphatidylinositol (PI) > sphingomyelin (SPH) > PS > diphosphatidylglycerol (DPG) > lysophosphatidylcholine (LPC). When cells were treated with *t*-BuOOH, no change in content of different classes of phospholipids in cells was found.

HL-60 cells readily incorporated PnA into the major phospholipid classes. The specific and relative incorporation of PnA into various phospholipid classes obtained from whole cells is shown in Table 3. When PnA content in whole cell-derived phospholipids was normalized relative to the amount of total lipid phosphorus, approximately 80% was found in PC and

17% was found in PE, reflecting the overall abundance of these phospholipids within cells (see Table 2). The specific content of PnA normalized to the amount of phosphorus in each phospholipid class ranged from 228.9 ng/mg of phosphorus in the PC fraction to 3.1 ng/mg of phosphorus in the SPH fraction. Note that despite the fact that PE is approximately five times more abundant relative to PS, the specific activity of PnA in PS is nearly 70% of that in PE (60.3 ng/mg of lipid phosphorus in the PS fraction versus 88.7 ng/mg of lipid phosphorus in the PE fraction). These differences most likely reflect differences in the metabolic turnover rate of each phospholipid class, as well as the overall composition of endogenous saturated and polyunsaturated fatty acids within individual phospholipid classes. The relative molar ratios of incorporated PnA:phospholipid for various lipid classes derived from whole cells were 1:39 for PC, 1:99 for PE, 1:146 for PS, 1:744 for DPG, 1:1,584 for PI, and 1:2,909 for SPH. Hence, only a very small fraction of each class of phospholipid becomes labeled with PnA and, thus, does not likely perturb the biophysical properties of cell membranes.

TABLE 3. INCORPORATION OF PNA INTO PHOSPHOLIPIDS OF INTACT CELLS AND VARIOUS SUBCELLULAR FRACTIONS ISOLATED FROM HL-60 CELLS

	DPG	PE	PC	SPH	PI	PS
Relative incorporation (ng of PnA/ $\mu$ g of total lipid phosphorus)						
HL-60 cells	3.9 ± 1.1	197.6 ± 17.0	940.0 ± 41.0	1.5 ± 0.1	3.0 ± 0.5	25.0 ± 2.5
Plasma membrane	5.4 ± 0.2	175.2 ± 3.5	662.8 ± 13.0	1.8 ± 0.1	1.6 ± 0.1	50.0 ± 0.4
Mitochondria	5.1 ± 0.2	192.8 ± 4.6	924.0 ± 28.6	1.2 ± 0.1	4.4 ± 0.2	10.9 ± 0.7
Microsomes	4.7 ± 0.1	218.8 ± 2.2	933.0 ± 53.0	1.7 ± 0.1	2.8 ± 0.1	40.2 ± 0.6
Nuclei	4.6 ± 0.2	232.0 ± 4.9	1,052.0 ± 16.8	1.0 ± 0.1	1.5 ± 0.2	10.1 ± 0.5
Lysosomes	3.1 ± 0.3	95.6 ± 3.5	426.0 ± 16.6	0.8 ± 0.1	2.6 ± 0.1	19.8 ± 1.0
Specific incorporation (ng of PnA/ $\mu$ g of lipid phosphorus in phospholipid fraction)						
HL-60 cells	97.4 ± 29.0	721.0 ± 62.0	1,861.0 ± 81.0	25.5 ± 2.3	45.5 ± 7.1	490.0 ± 55.0
Plasma membrane	158.9 ± 5.6	582.0 ± 12.0	1,578.0 ± 32.0	16.2 ± 1.2	82.4 ± 9.7	609.2 ± 5.4
Mitochondria	86.9 ± 3.5	717.0 ± 17.2	1,747.0 ± 54.2	44.4 ± 2.3	55.9 ± 1.3	353.0 ± 22.9
Microsomes	155.4 ± 4.0	801.4 ± 8.1	2,115.0 ± 57.0	19.7 ± 0.6	41.4 ± 2.1	528.5 ± 7.8
Nuclei	243.0 ± 12.1	745.0 ± 15.6	1,631.0 ± 26.1	24.9 ± 0.7	24.0 ± 3.8	457.0 ± 23.7
Lysosomes	43.4 ± 4.0	322.0 ± 11.9	1,014.0 ± 39.5	10.0 ± 0.3	40.0 ± 1.7	309.0 ± 15.5

Data represent means ± SEM (*n* = 6).



Figure 3 shows that significant oxidation of PnA was observed in SPH, PE, PS, and PC derived from whole cells. No significant oxidation of PnA was observed in DPG or PI. In keeping with our previous observations during oxidant-induced apoptosis (18–20), we observed that PS was by far the most sensitive to oxidation following exposure to *t*-BuOOH; nearly 60% of PnA-labeled PS was oxidized. The oxidation of PE, PC, and SPH did not exceed 24% and was similar among each class.

*Subcellular distribution of lipid peroxidation.* HPTLC analysis of phospholipids isolated from various subcellular fractions revealed a largely similar profile to those ex-

tracted from whole cells (Table 2). PC ranged from about 40 to 60% of the total phospholipid in the various fractions, with the greatest proportion recovered from nuclei. PE represented ~25–30% of total phospholipid in any fraction. Plasma membrane had a relatively high content of SPH, as did the lysosomal and microsomal fractions. SPH is known to be enriched in plasma membranes (71) and, accordingly, nuclei and mitochondria contained relatively little SPH. Small differences were also observed for PS where its distribution appeared to parallel that of SPH. Mitochondria and lysosomes were characterized by an elevated amount of DPG; its content in these fractions was two-fold higher compared with other subcellular fractions. PI content was approximately the same in all the subcellular fractions. Es-

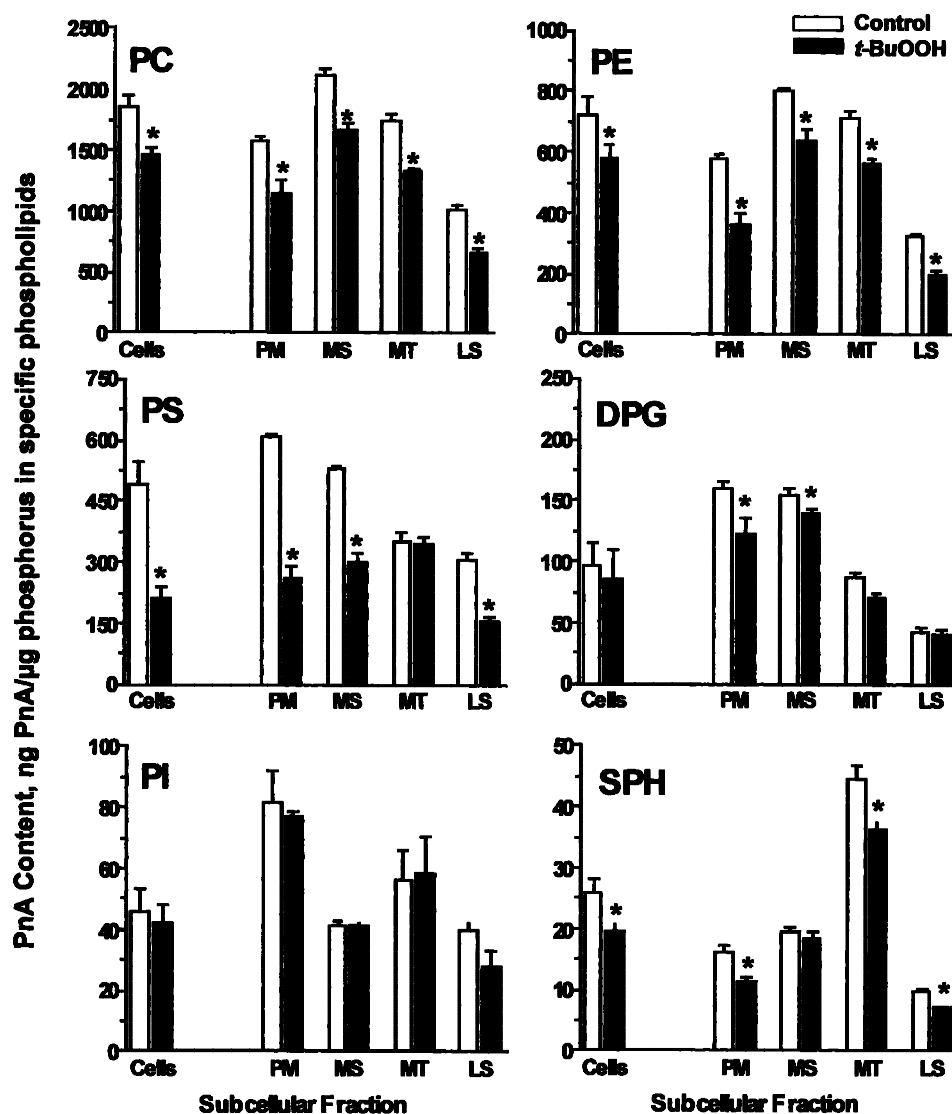


FIG. 3. *t*-BuOOH induced phospholipid oxidation in whole cells and subcellular fractions isolated from HL-60 cells. HL-60 cells were treated with PnA (2 μg of PnA/10<sup>6</sup> cells) in serum-free L-15 supplemented with glucose for 2 h at 37°C. PnA-labeled cells (2 × 10<sup>6</sup> cells) were incubated in the presence of *t*-BuOOH (150 μM) for 20 min at 37°C. Lipid oxidation was terminated by addition of 10 μM BHT, and cells were further processed as described in Materials and Methods. Lipids extracted from whole cells and subcellular organelles were resolved by HPLC and unoxidized PnA measured in each peak using an in-line fluorescence detector. Data are means ± SEM ( $n = 6$ ). \*Significant difference ( $p < 0.05$ ) relative to untreated controls. Cells, intact HL-60 cells; PM, plasma membrane; MS, microsomes; MT, mitochondria; LS, lysosomes.

essentially no significant difference in the pattern of distribution of the major phospholipid classes was observed between subcellular organelles isolated from control cells and cells treated with *t*-BuOOH. A small, but significant increase in content of LPC in plasma membrane, microsomes, and nuclei isolated from *t*-BuOOH-treated HL-60 cells was observed. It is known that oxidative stress can provoke hydrolysis of oxidized phospholipids as part of a deacylation/reacylation repair mechanism (50). To minimize any artifactual loss of PnA labeling due to phospholipid hydrolysis during cell fractionation, we maintained strict Ca<sup>2+</sup>-free conditions during the isolation procedure to inhibit Ca<sup>2+</sup>-dependent phospholipases. The paucity of LPC in all organelle fractions from untreated cells suggests that negligible phospholipid remodeling occurred during the isolation process.

Table 3 shows the content of PnA-labeled phospholipids in organelles normalized both to the amount of total phospholipid (relative content) and to the amount of lipid phosphorus in the particular phospholipid fraction (specific content). Table 3 clearly shows that when PnA labeling is expressed relative to total phospholipid phosphorus, the majority of PnA (~80% of total incorporated PnA) was incorporated into PC. This is similar to that observed in phospholipids derived from whole cells and reflects the relative abundance of this phospholipid in cells and organelles (see Table 2). Similarly, incorporation of PnA into PE ranged from 16.9% to 19.5% of total incorporation over various fractions. The most notable difference appeared with PS, where the incorporation of PnA was greatest in plasma membrane (nearly 6% of total PnA incorporated into this fraction) compared with other organelles. The rank order for PnA incorporation into PS for the remaining fractions was microsomes (3.3%) > lysosomes (3.6%) > mitochondria (1%) > nuclei (0.8%). The incorporation of PnA into DPG, PI, and SPH does not exceed 1% in subcellular fractions (Table 3).

If PnA incorporation is expressed relative to the phosphorus content of the specific lipid fraction, substantial differences in the specific activity of labeled phospholipids can be observed both between individual phospholipid classes and for a given phospholipid class between various organelles. For example, the highest specific activity in all fractions was achieved in PC and ranged from 40 to 100 times greater compared with incorporation into SPH. The specific activity of PS varied two-fold with the greatest specific activity clearly achieved in the plasma membrane fraction. The lowest rates of PnA incorporation into any phospholipid class were observed in the lysosomal fraction. As noted with whole cells, these differences probably reflect differences in synthesis/turnover rates in various phospholipids, as well as differences in fatty acid composition. Furthermore, differences observed between various organelle fractions may also reflect differences in rates of transport between intracellular sites of phospholipid synthesis and the various intracellular organelles.

Figure 3 shows the extent of PnA oxidation within various phospholipid classes observed in various subcellular fractions and its comparison with that observed in whole cells. It is clear that there are notable differences between various subcellular fractions in terms of their sensitivity to oxidation of specific phospholipids. First, the nuclear fraction was remarkably resistant to oxidation following *t*-BuOOH because no significant decrement in fluorescent content of PnA could be

detected in any phospholipid measured (data not shown). In general, the degree of PnA oxidation within PC, PE, and SPH from plasma membrane, microsomes, lysosomes, and mitochondria essentially resembled that observed in whole cells with ~20% being oxidized in all fractions. Exceptions to this were a 38% loss of PnA in PE derived from plasma membrane and lysosomes and a minimal (<6%) oxidation of SPH in microsomes. Therefore, these lipids, for the most part, were uniformly oxidized throughout most membrane compartments, a result that suggests a random lipid peroxidation process. In contrast, the amount of PnA oxidized in PS was much greater in plasma membrane where 57% of the fluorescence was lost following *t*-BuOOH. In addition, microsomal and lysosomal membranes also exhibited degrees of PS oxidation similar to that seen in whole cells with 43% and 50% oxidation, respectively. Moreover, PS within mitochondria was essentially resistant to oxidation, despite the fact that significant oxidation of PC, PE, and SPH could be observed in this fraction. Hence, the pattern of PS oxidation did not resemble the random process observed with the other major phospholipid classes. No oxidation of PI could be observed in any subcellular fraction, an observation similar to that seen in whole cells, and only modest oxidation of DPG was measurable in the plasma membrane (22.6%) and microsomal (11%) fractions.

The specific rate of PnA oxidation within each of the phospholipid classes was calculated and the results presented in Table 4. For PC, the oxidation rate was approximately the same in plasma membrane, microsomes, mitochondria, and lysosomes, and estimated to be 9.5, 9.9, 9.3, and 7.3 pmol of PnA/μg of PC phosphorus/min, respectively. In contrast, the rate of PS oxidation was 1.5 to two times greater in plasma membrane (7.7 pmol of PnA/μg of PS phosphorus/min) as compared with other organelles. It is noteworthy that the rate of PnA oxidation in PS approximates that observed in PC despite the fact that the specific activity of PnA incorporation is approximately fourfold less in PS. Plasma membrane PE was oxidized with a rate of 5.1 pmol of PnA/μg of PE phosphorus and was also 1.5- to twofold higher compared with that in microsomes, mitochondria, and lysosomes. The rate of PnA oxidation in DPG and SPH from all organelle fractions was much lower than observed for PS, PE, and PC and most likely re-

TABLE 4. OXIDATION RATE OF PNA-LABELED PHOSPHOLIPIDS IN INTACT CELLS AND SUBCELLULAR FRACTIONS ISOLATED FROM HL-60 CELLS

Subcellular fraction	Rate of PnA oxidation (pmol/μg of phosphorus in specific fraction/min)				
	PC	PS	PE	DPG	SPH
Whole cells	8.8	6.2	3.2	0.2	0.1
Plasma membrane	9.5	7.7	5.1	0.2	<0.1
Microsomes	9.9	5.0	3.5	0.4	0.1
Mitochondria	9.3	0.2	3.4	0.4	0.2
Lysosomes	7.3	3.4	2.7	<0.1	<0.1

The rate of *t*-BuOOH-induced oxidation of PnA was calculated as the difference between the specific PnA content of phospholipids in *t*-BuOOH-treated cells and that in control cells divided by 20 min.

flects the relatively low incorporation of PnA into these phospholipid classes. Similarly, the oxidation rate of PnA in PI did not exceed 0.25 pmol of PnA/ $\mu$ g of PI phosphorus/min in any organelle fraction (data not shown).

### Cytochrome *c*-induced oxidation of phospholipids

Our study demonstrated that apoptosis induced by *t*-BuOOH in HL-60 cells is associated with the release of cytochrome *c* from mitochondria into cytosol. As cytochrome *c* is a redox-active hemoprotein, we hypothesized that selective oxidation of PS may be mediated via the cytochrome *c*. To investigate the relationship between a release of cytochrome *c* and oxidation of PS, we measured the ability of exogenous cytochrome *c* to induce selective oxidation of PS in intact HL-60 cells. Using cells metabolically labeled with PnA, we incorporated cytochrome *c* into cells using gentle sonication and measured PnA oxidation in specific phospholipid classes after 20 min of incubation at 37°C. Cells were then incubated in the presence and absence of *t*-BuOOH (150  $\mu$ M) to determine if it was necessary to provide an oxidant such as *t*-BuOOH to permit initiation of cytochrome *c*/Fe-based redox activity. The percentage of PnA oxidation was determined relative to control cells that received the sonication treatment, but in the absence of cytochrome *c*. Figure 4A shows that cytochrome *c* alone incorporated into cells by mild sonication produced oxidation primarily in PS, where up to 20% of PS was oxidized at these conditions. The oxidation of other phospholipids did not exceed 8%. When cytochrome *c*-loaded cells were chal-

lenged with 150  $\mu$ M *t*-BuOOH (Fig. 4C), an increase in oxidation of all phospholipids was observed, but PS showed more oxidation compared with other phospholipids. *t*-BuOOH treatment of sonicated cells without incorporated cytochrome *c* (Fig. 4B) resulted in intermediate levels of lipid oxidation again with PS predominating similar to that seen earlier with naive HL-60 cells. The amount of incorporated cytochrome *c* was estimated spectrophotometrically (extinction coefficient,  $\epsilon_{553}^{\text{red}} = 15.3 \times 10^3 \text{ M}^{-1} \text{ cm}^{-1}$ ) and calculated to be  $0.44 \pm 0.03$  nmol/mg of protein (mean  $\pm$  SEM,  $n = 5$ ). Endogenous cytochrome *c* in control cells was essentially undetectable under these conditions.

We next tested our hypothesis in a cell-free model system to assess directly the potential of cytochrome *c* to mediate oxidation of select phospholipids. Multilamellar dispersions of 1-palmitoyl-2-arachidonoyl-*sn*-glycero-3-phosphoserine or with 1-palmitoyl-2-arachidonoyl-*sn*-glycero-3-phosphocholine were prepared and then incubated with ascorbate and  $\text{H}_2\text{O}_2$  for 1 h at 37°C. The extent of lipid peroxidation was then assessed by measuring the ratio of absorbance at 232 nm to absorbance at 205 nm, reflecting the formation of lipid hydroperoxides with conjugated dienes. Figure 5 shows the time-dependent formation of conjugated dienes in PS and PC under these incubation conditions. Incubation of PS with cytochrome *c* in combination with ascorbate/ $\text{H}_2\text{O}_2$  produced a robust fatty acid oxidation that was detected as early as 5 min and was increased over 10-fold after 1 h of incubation (Fig. 5, solid bars). No oxidation was observed in PS after incubation with ascorbate/ $\text{H}_2\text{O}_2$  alone, thus demonstrating the dependence of this effect on

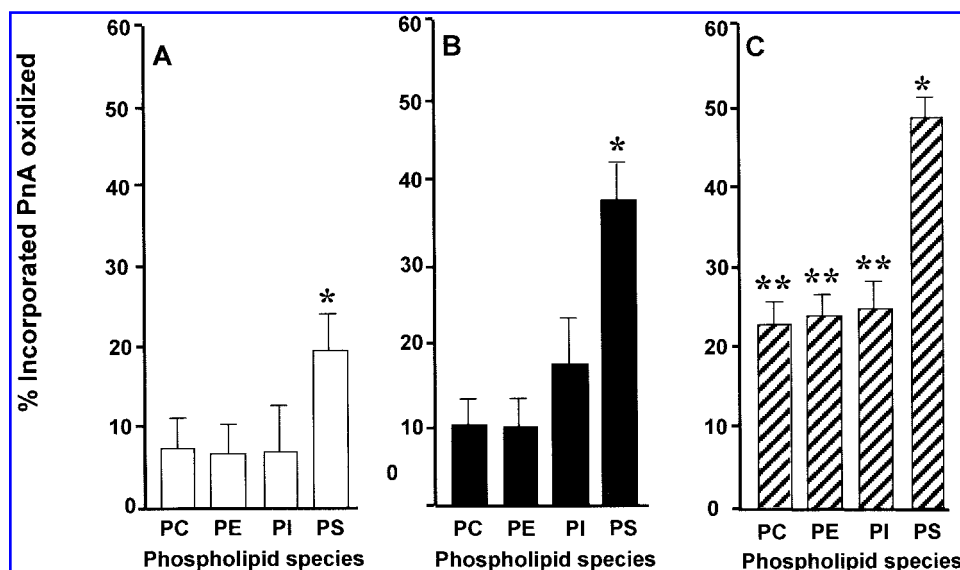


**FIG. 4. Effect of cytochrome *c* on *t*-BuOOH-induced phospholipid oxidation in HL-60 cells.** HL-60 cells were treated with PnA (2  $\mu$ g of PnA/ $10^6$  cells) in serum-free L-15 medium supplemented with glucose for 2 h at 37°C. Cytochrome *c* was incorporated into PnA-labeled cells by mild sonication as described in Materials and Methods. PnA-labeled cells ( $1 \times 10^6$  cells) loaded with cytochrome *c* were incubated in the presence (C) or absence (A) of *t*-BuOOH (150  $\mu$ M) for 20 min at 37°C. (B) Control cells sonicated without cytochrome *c* and treated with *t*-BuOOH. Lipids were extracted and resolved by HPLC as described above. The percentage of oxidized PnA in each phospholipid class was determined relative to the PnA content in phospholipids from control untreated cells that were sonicated in the absence of cytochrome *c*. Data represent means  $\pm$  SEM. \*Significant difference ( $p < 0.05$ ) relative to all other phospholipids as compared by Student's *t* test. \*\*Significant difference ( $p < 0.05$ ) relative to PI, PE, and PC, respectively, oxidized in the presence of cytochrome *c* alone or *t*-BuOOH alone.

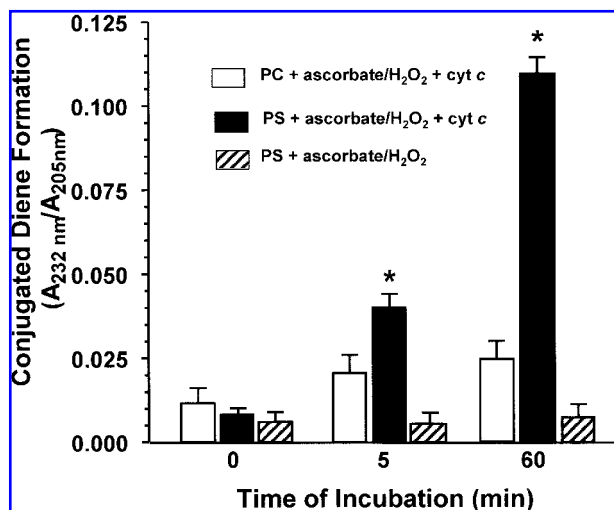


**FIG. 5. Cytochrome *c* mediates *in vitro* oxidation of PS, but not PC.** Multilamellar dispersions of PS or PC were prepared using 1-palmitoyl-2-arachidonyl-*sn*-glycero-3-phosphocholine or 1-palmitoyl-2-arachidonyl-*sn*-glycero-3-phospho-L-serine as described in Materials and Methods. PC (open bars) and PS (closed bars) lipid dispersions were incubated with 5  $\mu$ M cytochrome *c*, 500  $\mu$ M ascorbate, 400  $\mu$ M H<sub>2</sub>O<sub>2</sub>, and 100  $\mu$ M deferoxamine in 50 mM phosphate buffer (pH 7.4). Hatched bars represent PS incubated with all components except cytochrome *c*. Oxidation of PS and PC was assessed by measuring conjugated diene content ( $A_{232}/A_{205}$ ) in the total phospholipid extracts obtained at various times after incubation. \*Significant difference ( $p < 0.05$ ) compared with time 0 value using Student's *t* test.

cytochrome *c* (Fig. 5, hatched bars). This effect was specific for PS because cytochrome *c*-mediated oxidation of PC in the presence of *t*-BuOOH was not observed under identical conditions despite the similar composition of the polyunsaturated fatty acid in the *sn*-2 position (Fig. 5, open bars).

## DISCUSSION

### *t*-BuOOH-induced apoptosis is associated with selective oxidation of PS in the plasma membrane

Oxidative stress and the formation of various reactive oxygen species have been implicated as components of the final common pathway leading to the execution of apoptosis following exposure to tumor necrosis factor, growth factor withdrawal, various oxidants, and numerous other insults (10, 13, 38, 60, 78). We have recently reported that apoptosis following exposure to paraquat (18), 2',2'-azo-bis-2,4-dimethylvaleronitrile (an azo initiator of peroxy radicals) (19), or other stimuli (45, 69, 70) was associated with the selective oxidation of PS in several cell types. The significance of this phenomenon is underscored by the facts that PS oxidation was resistant to a vitamin E analogue and was attenuated by overexpression of bcl-2 (18, 19). These measurements, however, were performed using phospholipid extracts from whole cells and, hence, we could not directly assess the cellular localization where spe-

cific phospholipids were oxidized. Here we show that PS was again selectively oxidized above other phospholipids during *t*-BuOOH-induced apoptosis in HL-60 cells and, most importantly, that the plasma membrane was a favored site of PS oxidation.

It was clear that the greatest degree of overall oxidation was observed within the plasma membrane compartment (Fig. 3, Table 4). In addition, the "extra" oxidation relative to other compartments was largely contributed by enhanced oxidation of aminophospholipids, PS and PE. Interestingly, these two lipids are concentrated on the inner face of the cell membrane so the preferential oxidation is not simply a matter of preferential exposure of the plasma membrane to extracellularly applied *t*-BuOOH. Furthermore, many other intracellular compartments showed comparable rates of PC oxidation, indicating that diffusion does not severely limit the distribution of *t*-BuOOH to internal cellular locations.

It needs to be emphasized that *t*-BuOOH by itself does not possess significant oxidant activity, but initiates reactive oxygen species only by concerted action with specific catalysts, most notably, hemoproteins, iron-sulfur proteins, or other transition metal-containing proteins within cells (33). The abundance of these proteins in membrane-bound electron transport systems (mixed function oxidases, NADH/NADPH oxidoreductases, mitochondrial respiration) renders the lipids in cell membranes particularly sensitive to oxidative attack following *t*-BuOOH. One would predict, however, that oxidation would occur relatively randomly and that extent and rates of oxidation would primarily follow the relative abundance of each phospholipid class. This is clearly not the case here. The "random" pattern of oxidation observed in the mitochondria is unusual because only in this organelle does the rate of oxidation of each phospholipid follow its relative abundance (PC > PE >> PI = PS = DPG = SPH), with little, if any, oxidation being detected in the latter four phospholipids. In contrast, the pattern of oxidation in plasma membrane reveals a greater than expected oxidation of PS compared with other phospholipids. One explanation is that the specific intracellular iron-containing catalysts are not randomly distributed and in some way can direct the selective oxidation of specific phospholipid species. A notable hemoprotein is cytochrome *c*, whose cellular distribution changes during apoptosis and may allow its interaction with distant targets (see below). A similar effect is observed in microsomes and lysosomes, whose location would also allow potential interaction with cytochrome *c* only during apoptosis.

It has been demonstrated that aminophospholipid rearrangement within the plasma membrane takes place during the early stages of apoptosis (22, 44, 73, 79). This results in PS, and to some extent PE, translocation from the inner to the outer leaflet of membrane. Regulation of PS exposure in apoptosis does not appear to involve the participation of nuclear activity (22, 62). Oxidation of PS in plasma membrane may be functionally linked with PS externalization and subsequent phagocytosis. One of the putative cognate receptors on the surface macrophages that recognizes apoptotic cells appears related to "scavenger" receptors specific for oxidized low-density lipoprotein and, thus, suggests that oxidized PS on the surface of apoptotic cells may provide a better recognition signal than native PS (56, 74).

We have speculated that PS oxidation may also modulate the translocation process itself (35). Apparently, the accumulation of aminophospholipids (PE and PS) on the cell surface results from the concerted regulation of two particular membrane-bound enzymes termed phospholipid scramblase and APT (3, 4, 7, 79). Activation of the normally inactive phospholipid scramblase results in the bidirectional random movement of all phospholipid species within the membrane bilayer. In addition, inactivation of the constitutively active APT is also required to inhibit its surveillance function and permit PS accumulation on the cell surface. One possibility is that oxidized PS represents a substrate that is not recognized by APT. In addition, intimate association of the APT protein with reactive species of PS formed during the lipid peroxidation reaction could lead to functional modifications of its transporting capabilities. APT activity has previously been shown to be sensitive to oxidation and thiol modification (14, 29, 47). We have recently suggested that thiols in APT may represent hypersensitive targets during membrane-based oxidative/nitrosative stress in HL-60 cells (20).

### *Lipid oxidation in other organelles*

PnA oxidation in various phospholipid classes obtained from lysosomes and microsomes in general appeared to mimic the profile observed in whole cells and in plasma membrane. Large amounts of PS appeared to be oxidized, but not to the same extent as in plasma membrane. Other phospholipids appeared to be oxidized in a random manner that corresponds to their relative abundance. Membranes derived from nuclei and mitochondria showed some notable differences, and these are discussed in detail below.

**Nuclei.** Cell nuclei appeared relatively resistant to oxidation of any phospholipid class following *t*-BuOOH. Our assay does not depend on the composition of endogenous unsaturated fatty acids in this membrane, and PnA incorporation into major phospholipids in the nucleus was comparable to that observed in whole cells and other subcellular compartments. Therefore, the lack of oxidation observed cannot arise from lack of appropriate substrates in this region. The reason for low oxidation remains unknown, but most likely reflects a relatively low distribution of metal-containing proteins responsible for initiation of *t*-BuOOH-dependent oxidative stress. It is also possible that lipoprotective antioxidant mechanisms are particularly enriched within the nuclear membrane and serve to mitigate lipid peroxidation within this region. Given the close proximity to DNA and the need to preserve genetic material from oxidative damage, it may be important to minimize oxidative stress within the region.

**Mitochondria.** Changes in mitochondrial function, including their being a locus of oxidative stress, are now accepted as important during the execution of apoptosis (53). They serve as the source of cytochrome *c* that interacts with Apaf-1 and ATP to form the procaspase-activating apoptosome (11, 83); however, the mechanisms regulating cytochrome *c* release and generation of reactive oxygen species remain obscure. Activation of the permeability transition pore and subsequent depo-

larization of mitochondria are often observed early in apoptosis and have been implicated in the release of cytochrome *c* (53, 81).

In our study here, mitochondria did not show any preference for lipid oxidation in general above that seen in other organelle fractions, suggesting that they were not greater sources of reactive oxygen species than any other cellular location under these conditions. As mentioned above, the profile of lipid oxidation suggests a random process governed primarily by the relative abundance of each phospholipid class. PS was only minimally oxidized in keeping with the redistribution of cytochrome *c* away from mitochondria and into cytosol (see below). Thus, gross collapse of mitochondrial integrity with massive generation of oxidative stress was not apparent at this time. Similarly, Green and co-workers have quite elegantly demonstrated that cytochrome *c* release occurs independently of mitochondrial permeability transition (5), and collapse of inner mitochondrial transmembrane potential is not required for apoptosis (23).

The unique phospholipid, DPG or cardiolipin, is of special interest in these studies because mitochondria are especially rich in DPG. We indeed observed a twofold enrichment of DPG in our mitochondrial fraction compared with other fractions besides lysosomes. Although inefficiencies in separating lysosomes and mitochondria may lead to significant mitochondrial contamination within the lysosomal fraction, it is important to emphasize that the mitochondrial fraction was relatively free of  $\beta$ -galactosidase activity and, thus, comparatively pure. Using the fluorescent probe nonyl acridine orange (NAO), some workers have reported an early decrease in mitochondrial content of intact cardiolipin early in apoptosis (57, 76). It has been proposed that this loss represents oxidation of cardiolipin, a modification that could disrupt its high-affinity binding for cytochrome *c* and possibly aid in its release from mitochondria (67). In contrast, we failed to observe any changes in cardiolipin content or oxidation of PnA incorporated in mitochondrial DPG despite the fact that oxidation could be observed in other phospholipids (PC and PE). It should be pointed out that NAO binds to the alcoholic moieties in the CL polar head group and provides no information regarding the oxidation of fatty acid residues of the phospholipid (52). Our PnA assay, however, clearly measures oxidation of the unsaturated fatty acids representing the most likely physiological substrates during lipid peroxidation. Caspase activation was clearly evident by 1 h post exposure, suggesting that cytochrome *c* release had already occurred at an earlier time. Thus, oxidation of cardiolipin is not required (despite its being extremely sensitive to oxidative attack) for the events leading to plasma membrane PS oxidation or its externalization as measured by fluorescamine labeling during apoptosis.

### *Cytochrome c may mediate selective PS oxidation in apoptosis*

Cytochrome *c* release from mitochondria has recently been implicated as a component of apoptotic signaling (31, 39, 40, 61, 80). The mechanism of action in this role, however, has not been fully defined. The presence of iron within a heme moiety in cytochrome *c* suggests that this protein could catalyze the formation of reactive oxygen species (58). Although

it has been shown that the redox activity of cytochrome *c* is not required for its interaction with Apaf-1 and subsequent activation of caspase-3 (27, 40), these studies have not specifically addressed the effects on PS oxidation and externalization. As PS externalization can be biochemically dissociated from other end points of apoptosis (7, 82), we hypothesized that phospholipids could be targets for the redox action of cytochrome *c* action during apoptosis.

Cytochrome *c* is a basic protein that interacts with high affinity with anionic phospholipids, most notably PS (2, 15, 54). In fact, apocytochrome *c*/PS interactions have been implicated in the mitochondrial import of cytochrome *c* (2, 54, 64, 65). Numerous studies have demonstrated the potential of cytochrome *c* to catalyze peroxidation of different phospholipids in both liposomes and membrane fractions (25, 59). Combined, these data suggest that cytosolic cytochrome *c* may be involved in specific interaction with PS located in the cytosolic leaflet of the plasma membrane and be responsible for selective PS oxidation during apoptosis. It is particularly interesting that PS and PE showed the most robust oxidation in plasma membrane where they are primarily located on the inner membrane face and, thus, would be ideal targets for cytochrome *c*-dependent oxidation during apoptosis. In addition, these events appear to occur simultaneously within the first 20 min to 1 h of apoptosis induction following *t*-BuOOH.

We attempted to correlate more closely the appearance of cytochrome *c* in the cytosol temporally with the observed oxidation of PS using our western blot technique. We could not, however, consistently detect enhanced accumulation of immunologically reactive cytochrome *c* in the cytosolic fraction before the 2-h time point. It is possible that this immunological approach lacks the sensitivity to detect low levels of cytochrome *c* released at early time points. This idea is supported by the fact that caspase-3 activation, presumably a cytochrome *c*-dependent effect, could be detected 1 h earlier than the appearance of cytochrome *c* in the cytosol (Figs. 1C and 2). It is known that exquisitely small amounts of cytochrome *c* are sufficient for assembly of the functional apoptosome (48). It may also be that similarly minute amounts of cytochrome *c* are adequate to provide the catalytic activity necessary to oxidize phospholipids in the vicinity of cytochrome *c* binding to plasma membrane. In addition, the pool of cytochrome *c* released from mitochondria and bound to PS-rich plasma membrane would be ignored in analysis of the cytosolic fractions. Moreover, cytochrome *c* binding to PS or various protein partners can modulate its tertiary structure and thus, potentially, its immunoreactivity (55). Caspase-dependent enhancement of cytochrome *c* immunoreactivity has recently been reported in *Drosophila* during the early phases of apoptosis (77). Therefore, it is clear that further studies using more sensitive and specific methods to assess cytochrome *c* trafficking and its functional activity during apoptosis are warranted.

We were able to recapitulate site-selective oxidation of PS in cells when cytochrome *c* was incorporated intracellularly using gentle sonication. Although some oxidation of PS was observed in the presence of cytochrome *c* alone (which probably reflects some basal redox cycling inherent in the presence of an aerobic environment), oxidation of PS, as well as other phospholipids, was greater in the presence of the or-

ganic peroxide *t*-BuOOH. Therefore, it is proposed that heme iron in cytochrome *c* and endogenous peroxides can interact to produce oxidative stress by initiation of alkoxyl or hydroxyl radicals and/or formation of the reactive oxoferryl complex, both of which are capable of initiating lipid peroxidation (25, 26, 58, 59). It is known that mitochondria produce a variety of free radicals, including superoxide and  $H_2O_2$ , while undergoing permeability transition (63) or upon release of cytochrome *c* (10). It, therefore, appears that all the required substrates for the proposed reactions are available within proximity of the inner plasma membrane surface. The fact that selective PS oxidation was observed in the presence of *t*-BuOOH alone in no way precludes our hypothesis because we demonstrate here that exposure to *t*-BuOOH induces apoptosis in HL-60 cells, an event that presumably involves mitochondrial release of endogenous cytochrome *c*.

We show using a cell-free model system that cytochrome *c* can indeed catalyze the oxidation of polyunsaturated fatty acids contained in phospholipids. Most notably, the ability of PS to undergo oxidation markedly surpassed that of PC, despite the fact that the fatty acid profile in each phospholipid was identical. Therefore, the specificity of its action must have been determined by the nature of the polar head groups and most likely reflects an electrostatic interaction between the anionic phospholipid, PS, and the basic amino acids contained in cytochrome *c*.

In conclusion, we show that *t*-BuOOH-induced apoptosis in HL-60 cells is accompanied by early release of cytochrome *c* and the selective oxidation and externalization of PS. It appears that a significant proportion of the PS oxidized was within the plasma membrane, where we postulate that PS oxidation can modulate PS externalization. Lastly, we demonstrate the potential of cytochrome *c*, a proapoptotic mediator released from mitochondria, to catalyze PS-specific oxidation. Future studies will address the biochemical mechanism by which cytochrome *c* directs site-specific lipid oxidation in cells, as well as delineate the relationship between PS oxidation and its subsequent externalization.

## ACKNOWLEDGMENTS

This work was supported by NIH grant 1RO1 HL-70755-01.

## ABBREVIATIONS

APT, aminophospholipid translocase; BHT, butylated hydroxytoluene; *t*-BuOOH, *tert*-butyl hydroperoxide; DPG, diphosphatidylglycerol;  $H_2O_2$ , hydrogen peroxide; HPTLC, high-performance thin-layer chromatography; hSA, human serum albumin; LPC, lysophosphatidylcholine; mPE, fluorescamine-modified phosphatidylethanolamine; mPS, fluorescamine-modified phosphatidylserine; NAO, nonyl acridine orange; PC, phosphatidylcholine; PE, phosphatidylethanolamine; PI, phosphatidylinositol; PMSF, phenylmethylsulfonyl fluoride; PnA, *cis*-parinaric acid (Z-9, E-11, Z-15-octadecatetraenoic acid); PS, phosphatidylserine; RNase, ribonuclease; SPH, sphingomyelin; TEMPO, 2,2,6,6-tetramethylpiperidine-*N*-oxyl.

## REFERENCES

- Allen RT, Hunter WJ 3rd, and Agrawal DK. Morphological and biochemical characterization and analysis of apoptosis. *J Pharmacol Toxicol Methods* 37: 215–228, 1997.
- Berkhout TA, Rietveld A, and deKruijff B. Preferential lipid association and mode of penetration of apocytochrome *c* in mixed model membranes as monitored by tryptophanyl quenching using brominated phospholipids. *Biochim Biophys Acta* 897: 1–4, 1987.
- Bevers EM, Comfurius P, Dekkers DWC, Harmsma M, and Zwaal RFA. Transmembrane phospholipid distribution in blood cells: control mechanisms and pathophysiological significance. *Biol Chem* 379: 973–986, 1998.
- Bevers EM, Comfurius P, Dekkers DWC, and Zwaal RFA. Lipid translocation across the plasma membrane of mammalian cells. *Biochim Biophys Acta* 1439: 317–330, 1999.
- Bossy-Wetzel E, Newmeyer DD, and Green DR. Mitochondrial cytochrome *c* release in apoptosis occurs upstream of DEVD-specific activation and independently of mitochondrial transmembrane depolarization. *EMBO J* 17: 37–49, 1998.
- Bottcher CJF, Van Gent CM, and Pries C. A rapid and sensitive sub-micro phosphorous determination. *Anal Chim Acta* 24: 203–204, 1961.
- Bratton DL, Fadok VA, Richter DA, Kailey JM, Guthrie LA, and Henson PM. Appearance of phosphatidylserine on apoptotic cells requires calcium-mediated nonspecific flip-flop and is enhanced by loss of aminophospholipid translocase. *J Biol Chem* 272: 26159–26165, 1997.
- Bruckheimer EM and Schroit AJ. Membrane phospholipid asymmetry: host response to the externalization of phosphatidylserine. *J Leukoc Biol* 59: 784–788, 1996.
- Budavari S. *The Merck Index*, 11th ed. Rahway, NJ: Merck & Co., Inc., 1989.
- Buttke TM and Sandstrom PA. Oxidative stress as a mediator of apoptosis. *Immunol Today* 15: 7–10, 1994.
- Cain K, Bratton SB, Langlais C, Walker G, Brown DG, Sun X-M, and Cohen GM. Apaf-1 oligomerizes into biologically active approximately 700-kDa and inactive approximately 1.4-MDa apoptosome complexes. *J Biol Chem* 275: 6067–6070, 2000.
- Cesarone CF, Bolognesi C, and Santi L. Improved microfluorometric DNA determination in biological material using 33258 Hoescht. *Anal Biochem* 100: 188–197, 1979.
- Chandra J, Samali A, and Orrenius S. Triggering and modulation of apoptosis by oxidative stress. *Free Radic Biol Med* 29: 323–333, 2000.
- de Jong K, Geldwerth D, and Kuypers FA. Oxidative damage does not alter membrane phospholipid asymmetry in human erythrocytes. *Biochemistry* 36: 6768–6776, 1997.
- Demel RA, Jordi W, Lambrechts H, van Damme H, Hovius R, and de Kruijff B. Differential interactions of apo- and holocytochrome *c* with acidic membrane lipids in model systems and the implications for their import into mitochondria. *J Biol Chem* 264: 3988–3997, 1989.
- Dolis D, Moreau C, Zachowski A, and Devaux PF. Aminophospholipid translocase and proteins involved in transmembrane phospholipid traffic. *Biophys Chem* 68: 221–231, 1997.
- Enari M, Talanian RV, Wong WW, and Nagata S. Sequential activation of ICE-like proteases during Fas-mediated apoptosis. *Nature* 380: 723–726, 1996.
- Fabisiak JP, Kagan VE, Ritov VB, Johnson DE, and Lazo JS. Bcl-2 inhibits selective oxidation and externalization of phosphatidylserine during paraquat-induced apoptosis. *Am J Physiol* 272: C675–C684, 1997.
- Fabisiak JP, Tyurina YY, Tyurin VA, Lazo JS, and Kagan VE. Random versus selective membrane oxidation in apoptosis: role of phosphatidylserine. *Biochemistry* 37: 13781–13790, 1998.
- Fabisiak JP, Tyurin VA, Tyurina YY, Sedlov A, Lazo JS, and Kagan VE. Nitric oxide dissociates lipid oxidation from apoptosis and phosphatidylserine externalization during oxidative stress. *Biochemistry* 39: 127–138, 2000.
- Fadeel B, Gleiss B, Hogstrand K, Chandra J, Wiedmer T, Sims PJ, Henter JJ, Orrenius S, and Samali A. Phosphatidylserine exposure during apoptosis is a cell-type-specific event and does not correlate with plasma membrane phospholipid scramblase expression. *Biochem Biophys Res Commun* 266: 504–511, 1999.
- Fadok V, Voelker DR, Campbell PA, Cohen JJ, Bratton DL, and Henson PM. Exposure of phosphatidylserine on the surface of apoptotic lymphocytes triggers specific recognition and removal by macrophages. *J Immunol* 148: 2207–2216, 1992.
- Finucane DM, Waterhouse NJ, Amarante-Mendes GP, Cotter TG, and Green DR. Collapse of the inner mitochondrial transmembrane potential is not required for apoptosis in HL-60 cells. *Exp Cell Res* 251: 166–174, 1999.
- Frey T. Correlated flow cytometric analysis of terminal events in apoptosis reveals absence of some changes in some model systems. *Cytometry* 28: 253–263, 1997.
- Galaris D, Sevanian A, Cadenas E, and Hochstein P. Ferrylmyoglobin-catalyzed linoleic acid peroxidation. *Arch Biochem Biophys* 281: 163–169, 1990.
- Gorbunov N, Osipov A, Day B, Zayas B, Kagan VE, and Elsayed N. Reduction of ferrylmyoglobin and ferrylhemoglobin by nitric oxide: a protective mechanism against ferrylhemoprotein-induced oxidations. *Biochemistry* 34: 6689–6699, 1995.
- Hampton MB, Zhivotovsky B, Slater AFG, Burgess DH, and Orrenius S. Importance of the redox state of cytochrome *c* during caspase activation in cytosolic extracts. *Biochem J* 329: 95–99, 1998.
- Henson PM, Bratton DL, and Fadok VA. Apoptotic cell removal. *Curr Biol* 11: R795–R805, 2001.
- Herrmann A and Devaux PF. Alteration of the aminophospholipid translocase activity in vivo and artificial aging of human erythrocytes. *Biochim Biophys Acta* 1027: 41–46, 1990.
- Ishikura H, Honma Y, Honma C, Hozumi M, Black JD, Kieber-Emmons T, and Bloch A. Inhibition of messenger RNA transcriptional activity in ML-1 human myeloblastic leukemia cell nuclei by antiserum to a c-myb-specific peptide. *Cancer Res* 47: 1052–1057, 1987.

31. Jiang X and Wang X. Cytochrome *c* promotes caspase-9 activation by inducing nucleotide binding to Apaf-1. *J Biol Chem* 275: 31199–31203, 2000.
32. Johannesen K, Depierre JW, Bergstrand A, Dallner G, and Ernster L. Preparation and characterization of total, rough, and smooth microsomes from the lung of control and methylcholanthrene-treated rats. *Biochim Biophys Acta* 496: 115–135, 1977.
33. Kagan VE. *Lipid Peroxidation of Biological Membranes*. Boca Raton, FL: CRC Press, 1988.
34. Kagan VE, Ritov VB, Tyurina YY, and Tyurin VA. Sensitive and specific fluorescent probing of oxidative stress in different classes of membrane phospholipids in live cells using metabolically integrated *cis*-parinaric acid. *Methods Mol Biol* 108: 71–87, 1998.
35. Kagan VE, Fabisiak JP, Shvedova AA, Tyurina YY, Tyurin VA, Schor NF, and Kawai K. Oxidative signaling pathway for externalization of plasma membrane phosphatidylserine during apoptosis. *FEBS Lett* 477: 1–7, 2000.
36. Kagan VE, Gleiss B, Tyurina YY, Tyurin VA, Elenstrom-Magnusson C, Liu S-X, Serinkan FB, Arroyo A, Chandra J, Orrenius S, and Fadeel B. A role of oxidative stress in apoptosis: oxidation and externalization of phosphatidylserine is required for macrophage clearance of cells undergoing Fas-mediated apoptosis. *J Immunol* 169: 487–499, 2002.
37. Kagan VE, Borisenko GG, Serinkan BF, Tyurina YY, Tyurin VA, Jiang J, Liu S-X, Shvedova AA, Fabisiak JP, Uthaisang W, and Fadeel B. Appetizing rancidity of apoptotic cells for macrophages: oxidation/externalization/recognition of phosphatidylserine. *Am J Physiol Lung Cell Mol Physiol* 285: L1–L17, 2003.
38. Kane DJ, Sarafian TA, Anton R, Hahn H, Gralla EB, Valentine JS, Ord T, and Bredesen DE. Bcl-2 inhibition of neural death: decreased generation of reactive oxygen species. *Science* 262: 1274–1277, 1993.
39. Kluck RM, Bossy-Wetzel E, Green DT, and Newmeyer DD. The release of cytochrome *c* from mitochondria: a primary site for Bcl-2 regulation of apoptosis. *Science* 275: 1132–1136, 1997.
40. Kluck RM, Martin SJ, Hoffman BM, Zhou JS, Green DR, and Newmeyer DD. Cytochrome *c* activation of CPP32-like proteolysis plays a critical role in a *Xenopus* cell-free apoptosis system. *EMBO J* 16: 4639–4649, 1997.
41. Kroemer G, Dallaporta B, and Resche-Rigon M. The mitochondrial death/life regulators in apoptosis and necrosis. *Annu Rev Physiol* 60: 619–642, 1998.
42. Liu X, Kim CN, Yang J, Jemmerson R, and Wang X. Induction of apoptotic program in cell-free extracts. *Cell* 86: 147–157, 1996.
43. Martin OC and Pagano RE. Transbilayer movement of fluorescent analogs of phosphatidylserine and phosphatidylethanolamine at the plasma membrane of cultured cells. Evidence for a protein-mediated and ATP-dependent process(es). *J Biol Chem* 262: 5890–5898, 1987.
44. Martin SJ, Reutelingsperger CPM, McGahon AJ, Rader JA, van Schie RC, LaFace DM, and Green DR. Early redistribution of plasma membrane phosphatidylserine is a general feature of apoptosis regardless of the initiating stimulus: inhibition by overexpression of Bcl-2 and Abl. *J Exp Med* 182: 1545–1556, 1995.
45. Maulik N, Kagan VE, Tyurin VA, and Das DK. Redistribution of phosphatidylethanolamine and phosphatidylserine precedes reperfusion-induced apoptosis. *Am J Cell Physiol* 274: H242–H248, 1998.
46. Miura M, Zhu H, Rotello R, Hartwig EA, and Yuan J. Induction of apoptosis in fibroblasts by IL-1 $\beta$ -converting enzyme, a mammalian homolog of the *C. elegans* cell death gene *ced-3*. *Cell* 75: 653–660, 1993.
47. Morrot G, Herve P, Zachowski A, Fellman P, and Devaux PF. Aminophospholipid translocase of human erythrocytes: phospholipid substrate specificity and effect of cholesterol. *Biochemistry* 28: 3456–3462, 1989.
48. Murphy BM, O'Neill AJ, Adrian C, Watson RWG, and Martin SJ. The apoptosome pathway to caspase activation in primary human neutrophils exhibits dramatically reduced requirement for cytochrome *c*. *J Exp Med* 197: 625–632, 2003.
49. Nicholson DW, Ali A, Thornberry NA, Vaillancourt JP, Ding CK, Gallant M, Gareau Y, Griffin PR, Labelle M, Lazebnik YA, Munday NA, Raju SM, Smulson ME, Yamin T-T, Yu VL, and Miller DK. Identification and inhibition of the ICE/CED-3 protease necessary for mammalian apoptosis. *Nature* 376: 37–43, 1995.
50. Pacifici EH, McLeod LL, and Sevanian A. Lipid hydroperoxide-induced peroxidation and turnover of endothelial cell phospholipids. *Free Radic Biol Med* 17: 297–309, 1994.
51. Patel T, Gores GJ, and Kaufmann SH. The role of proteases during apoptosis. *FASEB J* 10: 587–597, 1996.
52. Petit JM, Maftah A, Ratinaud MH, and Julien R. 10-N-nonyl acridine orange interacts with cardiolipin and allows the quantification of this phospholipid in isolated mitochondria. *Eur J Biochem* 209: 267–273, 1992.
53. Petit PX, LeCouer H, Zorn E, Daugnet C, Mignotte B, and Gougeon ML. Alterations in mitochondrial structure and function are early events of dexamethasone-induced thymocyte apoptosis. *J Cell Biol* 130: 157–167, 1995.
54. Pinheiro TJ and Watts A. Lipid specificity in the interaction of cytochrome *c* with anionic phospholipid bilayers revealed by solid-state  $^{31}\text{P}$  NMR. *Biochemistry* 33: 2451–2458, 1994.
55. Pinheiro TJ, Elove GA, Watts A, and Roder H. Structural and kinetic description of cytochrome *c* unfolding induced by interaction with lipid vesicles. *Biochemistry* 36: 13122–13132, 1997.
56. Platt N, Suzuki H, Kurihara Y, Kodama T, and Gordon S. Role for the class A macrophage scavenger receptor in the phagocytosis of apoptotic thymocytes in vitro. *Proc Natl Acad Sci U S A* 93: 12456–12460, 1996.
57. Polyak K, Xia J, Zweier JL, Kinzler KW, and Vogelstein B. A model for p53-induced apoptosis. *Nature* 389: 300–305, 1997.
58. Radi R, Turrens JF, and Freeman BA. Cytochrome *c*-catalyzed membrane lipid peroxidation by hydrogen peroxide. *Arch Biochem Biophys* 288: 118–125, 1991.
59. Radi R, Bush KM, and Freeman BA. The role of cytochrome *c* and mitochondrial catalase in hydroperoxide-induced heart mitochondrial lipid peroxidation. *Arch Biochem Biophys* 300: 409–415, 1993.
60. Raha S and Robinson BH. Mitochondria, oxygen free radicals, and apoptosis. *Am J Med Genet* 106: 62–70, 2001.



61. Reed JC. Cytochrome *c*: can't live with it—can't live without it. *Cell* 9: 559–562, 1997.
62. Reno F, Burattini S, Rossi S, Luchetti F, Columbaro M, Santi S, Papa S, and Falcieri E. Phospholipid rearrangement of apoptotic membrane does not depend on nuclear activity. *Histochem Cell Biol* 110: 467–476, 1998.
63. Richter C and Kass GEN. Oxidative stress in mitochondria: its relationship to cellular  $\text{Ca}^{2+}$  homeostasis, cell death, proliferation, and differentiation. *Chem Biol Interact* 77: 1–23, 1991.
64. Rietveld A, Berkhout TA, Roenhorst A, Marsh D, and de Kruijff B. Preferential association of apocytochrome *c* with negatively charged phospholipids in mixed model membranes. *Biochim Biophys Acta* 858: 38–46, 1986.
65. Rietveld A, Jordi W, and de Kruijff B. Studies on the lipid dependency and mechanism of the translocation of the mitochondrial precursor protein apocytochrome *c* across model membranes. *J Biol Chem* 261: 3846–3856, 1986.
66. Ritov VB, Banni S, Yalowich JC, Day BW, Claycamp HG, Corongiu FP, and Kagan VE. Non-random peroxidation of different classes of membrane phospholipids in live cells detected by metabolically integrated *cis*-parinaric acid. *Biochim Biophys Acta* 1283: 127–149, 1996.
67. Rytomaa M and Kinnunen PK. Reversibility of the binding of cytochrome *c* to liposomes. *J Biol Chem* 270: 3197–3202, 1995.
68. Savill J and Fadok V. Corpse clearance defines the meaning of death. *Nature* 407: 784–788, 2000.
69. Schor NF, Tyurina YY, Fabisiak JP, Tyurin VA, Lazo JS, and Kagan VE. Selective oxidation and externalization of membrane phosphatidylserine: Bcl-2-induced potentiation of the final common pathway for apoptosis. *Brain Res* 831: 125–130, 1999.
70. Shvedova AA, Tyurina YY, Kawai K, Tyurin VA, Kommineni C, Castranova V, Fabisiak JP, and Kagan VE. Selective peroxidation and externalization of phosphatidylserine in normal human epidermal keratinocytes during oxidative stress induced by cumene hydroperoxide. *Invest Dermatol* 118: 1008–1018, 2002.
71. Stoffel W. Sphingolipids. *Annu Rev Biochem* 40: 57–82, 1971.
72. Storrie M and Madden EA. Isolation of subcellular organelles. *Methods Enzymol* 182: 203–205, 1990.
73. Stuart MC, Damoiseaux JG, Frederik PM, Arends JW, and Reutelingsperger CP. Surface exposure of phosphatidylserine during apoptosis of rat thymocytes precedes nuclear changes. *Eur J Cell Biol* 76: 77–83, 1998.
74. Terpestra V, Kondratenko N, and Steinberg D. Macrophages lacking scavenger receptor A show a decrease in binding and uptake of acetylated low-density lipoprotein and apoptotic thymocytes, but not oxidatively damaged red blood cells. *Proc Natl Acad Sci U S A* 94: 8127–8131, 1997.
75. Thornberry NA, Rano TA, Peterson EP, Rasper DM, Timkey T, Garcia-Calvo M, Houtzager VM, Nordstrom PA, Roy S, Vaillancourt JP, Chapman KT, and Nicholson DW. A combinatorial approach defines specificities of members of the caspase family and granzyme B. Functional relationships established for key mediators of apoptosis. *J Biol Chem* 272: 17907–17911, 1997.
76. Ushmorov A, Ratter F, Lehmann V, Droge W, Schirmacher V, and Umansky V. Nitric oxide-induced apoptosis in human leukemic lines requires mitochondrial lipid degradation and cytochrome *c* release. *Blood* 93: 2342–2352, 1999.
77. Varkey J, Chen P, Jemmerson R, and Abrams JM. Altered cytochrome *c* display precedes apoptotic death in *Drosophila*. *J Cell Biol* 144: 701–710, 1999.
78. Verhagen S, McGowan AJ, Brophy AR, Fernandes RS, and Cotter T. Inhibition of apoptosis by antioxidants in the human HL-60 leukemia cell line. *Biochem Pharmacol* 50: 1021–1029, 1995.
79. Verhoven B, Schlegel RA, and Williamson P. Mechanisms of phosphatidylserine exposure, a phagocyte signal, on apoptotic T lymphocytes. *J Exp Med* 182: 1597–1601, 1995.
80. Yang J, Liu X, Bhalla K, Kim CN, Ibrado AM, Cai J, Peng T-I, Jones DP, and Wang X. Prevention of apoptosis by Bcl-2: release of cytochrome *c* from mitochondria blocked. *Science* 275: 1129–1132, 1997.
81. Zamzami N, Marchetti P, Castedo M, Decaudin D, Macho A, Hirsch T, Susin SA, Petit PX, Mignotte B, and Kroemer G. Sequential reduction of mitochondrial transmembrane potential and generation of reactive oxygen species in early programmed cell death. *J Exp Med* 182: 367–377, 1995.
82. Zhaung J, Ren Y, Snowden RT, Zhu H, Gogvadze V, Savill JS, and Cohen GM. Dissociation of phagocyte recognition of cells undergoing apoptosis from other features of the apoptotic program. *J Biol Chem* 273: 15628–15632, 1998.
83. Zou H, Li Y, Liu X, and Wang X. An APAF-1-cytochrome *c* multimeric complex is a functional apoptosome that activates procaspase-9. *J Biol Chem* 274: 11549–11556, 1999.

Address reprint requests to:

James P. Fabisiak

Department of Environmental and Occupational Health

School of Public Health

University of Pittsburgh

3343 Forbes Ave.

Pittsburgh, PA 15260

E-mail: fabs+@pitt.edu

Received for publication September 30, 2003; accepted November 10, 2003.

**This article has been cited by:**

1. Valerian Kagan, Anna Shvedova, Yulia Tyurina Healthy Free Radical Pessimism **30**, 3-12. [[CrossRef](#)]
2. Anna A. Shvedova, Antonio Pietroiusti, Bengt Fadeel, Valerian E. Kagan. 2012. Mechanisms of carbon nanotube-induced toxicity: Focus on oxidative stress. *Toxicology and Applied Pharmacology* **261**:2, 121-133. [[CrossRef](#)]
3. Yulia Y. Tyurina, Elena R. Kisin, Ashley Murray, Vladimir A. Tyurin, Valentina I. Kapralova, Louis J. Sparvero, Andrew A. Amoscato, Alejandro K. Samhan-Arias, Linda Swedin, Riitta Lahesmaa, Bengt Fadeel, Anna A. Shvedova, Valerian E. Kagan. 2011. Global Phospholipidomics Analysis Reveals Selective Pulmonary Peroxidation Profiles upon Inhalation of Single-Walled Carbon Nanotubes. *ACS Nano* 110804115816010. [[CrossRef](#)]
4. Angela Gambelunghé, Sandra Buratta, Giuseppina Ferrara, Rita Mozzi, Cristina Marchetti, Nicola Murgia, Giacomo Muzi. 2011. Phosphatidylserine Metabolism in Human Lymphoblastic Cells Exposed to Chromium (VI). *Journal of Occupational and Environmental Medicine* **53**:7, 776-781. [[CrossRef](#)]
5. Jacob Zabicky Analytical and Safety Aspects of Organic Peroxides and Related Functional Groups . [[CrossRef](#)]
6. Vladimir A. Tyurin, Yulia Y. Tyurina, Mi-Yeon Jung, Muhammad A. Tungekar, Karla J. Wasserloos, Hülya Bay#r, Joel S. Greenberger, Patrick M. Kochanek, Anna A. Shvedova, Bruce Pitt. 2009. Mass-spectrometric analysis of hydroperoxy- and hydroxy-derivatives of cardiolipin and phosphatidylserine in cells and tissues induced by pro-apoptotic and pro-inflammatory stimuli###. *Journal of Chromatography B* **877**:26, 2863-2872. [[CrossRef](#)]
7. Valerian E. Kagan, Hülya A. Bay#r, Natalia A. Belikova, Olexandr Kapralov, Yulia Y. Tyurina, Vladimir A. Tyurin, Jianfei Jiang, Detcho A. Stoyanovsky, Peter Wipf, Patrick M. Kochanek, Joel S. Greenberger, Bruce Pitt, Anna A. Shvedova, Grigory Borisenko. 2009. Cytochrome c/cardiolipin relations in mitochondria: a kiss of death. *Free Radical Biology and Medicine* **46**:11, 1439-1453. [[CrossRef](#)]
8. Vladimir A. Tyurin, Yulia Y. Tyurina, Weihong Feng, Alexandra Mnuskin, Jianfei Jiang, Minke Tang, Xiaojing Zhang, Qing Zhao, Patrick M. Kochanek, Robert S. B. Clark, Hülya Bay#r, Valerian E. Kagan. 2008. Mass-spectrometric characterization of phospholipids and their primary peroxidation products in rat cortical neurons during staurosporine-induced apoptosis. *Journal of Neurochemistry* **107**:6, 1614-1633. [[CrossRef](#)]
9. J JIANG, Z HUANG, Q ZHAO, W FENG, N BELIKOVA, V KAGAN. 2008. Interplay between bax, reactive oxygen species production, and cardiolipin oxidation during apoptosis. *Biochemical and Biophysical Research Communications* **368**:1, 145-150. [[CrossRef](#)]
10. Jeffrey Atkinson, Raquel F. Epand, Richard M. Epand. 2008. Tocopherols and tocotrienols in membranes: A critical review. *Free Radical Biology and Medicine* **44**:5, 739-764. [[CrossRef](#)]
11. Albert W. Girotti. 2008. Translocation as a means of disseminating lipid hydroperoxide-induced oxidative damage and effector action. *Free Radical Biology and Medicine* **44**:6, 956-968. [[CrossRef](#)]
12. Yulia Y. Tyurina, Vladimir A. Tyurin, Michael W. Epperly, Joel S. Greenberger, Valerian E. Kagan. 2008. Oxidative lipidomics of #-irradiation-induced intestinal injury. *Free Radical Biology and Medicine* **44**:3, 299-314. [[CrossRef](#)]
13. N BELIKOVA, J JIANG, Y TYURINA, Q ZHAO, M EPPERLY, J GREENBERGER, V KAGAN. 2007. Cardiolipin-Specific Peroxidase Reactions of Cytochrome c in Mitochondria During Irradiation-Induced Apoptosis. *International Journal of Radiation OncologyBiologyPhysics* **69**:1, 176-186. [[CrossRef](#)]
14. M KAPISZEWSKA, A CIERNIAK, M ELAS, A LANKOFF. 2007. Lifespan of etoposide-treated human neutrophils is affected by antioxidant ability of quercetin. *Toxicology in Vitro* **21**:6, 1020-1030. [[CrossRef](#)]

15. Jeng-Hsiung F. Peng, Yangzheng Feng, Philip G. Rhodes. 2006. Down-regulation of Phospholipase D2 mRNA in Neonatal Rat Brainstem and Cerebellum after Hypoxia-Ischemia. *Neurochemical Research* **31**:10, 1191-1196. [[CrossRef](#)]
16. H. Bayir, B. Fadeel, M.J. Palladino, E. Witas, I.V. Kurnikov, Y.Y. Tyurina, V.A. Tyurin, A.A. Amoscato, J. Jiang, P.M. Kochanek, S.T. DeKosky, J.S. Greenberger, A.A. Shvedova, V.E. Kagan. 2006. Apoptotic interactions of cytochrome c: Redox flirting with anionic phospholipids within and outside of mitochondria. *Biochimica et Biophysica Acta (BBA) - Bioenergetics* **1757**:5-6, 648-659. [[CrossRef](#)]
17. Yi Wu, Nitu Tibrewal, Raymond B. Birge. 2006. Phosphatidylserine recognition by phagocytes: a view to a kill. *Trends in Cell Biology* **16**:4, 189-197. [[CrossRef](#)]
18. Valerian E Kagan, Vladimir A Tyurin, Jianfei Jiang, Yulia Y Tyurina, Vladimir B Ritov, Andrew A Amoscato, Anatoly N Osipov, Natalia A Belikova, Alexandr A Kapralov, Vidisha Kini, Irina I Vlasova, Qing Zhao, Meimei Zou, Peter Di, Dimitry A Svistunenko, Igor V Kurnikov, Gregory G Borisenko. 2005. Cytochrome c acts as a cardiolipin oxygenase required for release of proapoptotic factors. *Nature Chemical Biology* **1**:4, 223-232. [[CrossRef](#)]
19. Valerian E. Kagan, Grigory G. Borisenko, Yulia Y. Tyurina, Vladimir A. Tyurin, Jianfei Jiang, Alla I. Potapovich, Vidisha Kini, Andrew A. Amoscato, Yasu Fujii. 2004. Oxidative lipidomics of apoptosis: redox catalytic interactions of cytochrome c with cardiolipin and phosphatidylserine. *Free Radical Biology and Medicine* **37**:12, 1963-1985. [[CrossRef](#)]
20. Valerian E. Kagan, Peter J. Quinn. 2004. Toward Oxidative Lipidomics of Cell Signaling. *Antioxidants & Redox Signaling* **6**:2, 199-202. [[Abstract](#)] [[Full Text PDF](#)] [[Full Text PDF with Links](#)]